



Trace element and Sr-Nd-Pb isotope geochemistry of Rungwe Volcanic Province, Tanzania: implications for a Superplume source for East Africa Rift magmatism

Paterno R. Castillo*, David R. Hilton and Sæmundur A. Halldórsson†

Geosciences Research Division, Scripps Institution of Oceanography, University of California, San Diego, La Jolla, CA, USA

Edited by:

Shuguang Song, Peking University, China

Reviewed by:

Yigang Xu, Chinese Academy of Sciences, China

William M. White, Cornell University, USA

*Correspondence:

Paterno R. Castillo, Geosciences Research Division, Scripps Institution of Oceanography, University of California, San Diego, 8615 Kennel Way, La Jolla, CA 92037, USA
e-mail: pcastillo@ucsd.edu

† Present address:

Sæmundur A. Halldórsson, Nordic Volcanological Center, Institute of Earth Sciences, University of Iceland, Reykjavik, Iceland

The recently-discovered high, plume-like $^3\text{He}/^4\text{He}$ ratios at Rungwe Volcanic Province (RVP) in southern Tanzania, similar to those at the Main Ethiopian Rift in Ethiopia, strongly suggest that magmatism associated with continental rifting along the entire East African Rift System (EARS) has a deep mantle contribution (Hilton et al., 2011). New trace element and Sr-Nd-Pb isotopic data for high $^3\text{He}/^4\text{He}$ lavas and tephros from RVP can be explained by binary mixing relationships involving Early Proterozoic (\pm Archaean) lithospheric mantle, present beneath the southern EARS, and a volatile-rich carbonatitic plume with a limited range of compositions and best represented by recent Nyiragongo lavas from the Virunga Volcanic Province also in the Western Rift. Other lavas from the Western Rift and from the southern Kenyan Rift can also be explained through mixing between the same endmember components. In contrast, lavas from the northern Kenyan and Main Ethiopian rifts can be explained through variable mixing between the same mantle plume material and Middle to Late Proterozoic lithospheric mantle, present beneath the northern EARS. Thus, we propose that the bulk of EARS magmatism is sourced from mixing among three endmember sources: Early Proterozoic (\pm Archaean) lithospheric mantle, Middle to Late Proterozoic lithospheric mantle and a volatile-rich carbonatitic plume with a limited range of compositions. We propose further that the African Superplume, a large, seismically anomalous feature originating in the lower mantle beneath southern Africa, influences magmatism throughout eastern Africa with magmatism at RVP and the Main Ethiopian Rift representing two different heads of a single mantle plume source. This is consistent with a single mantle plume origin of the coupled He-Ne isotopic signatures of mantle-derived xenoliths and/or lavas from all segments of the EARS (Halldórsson et al., 2014).

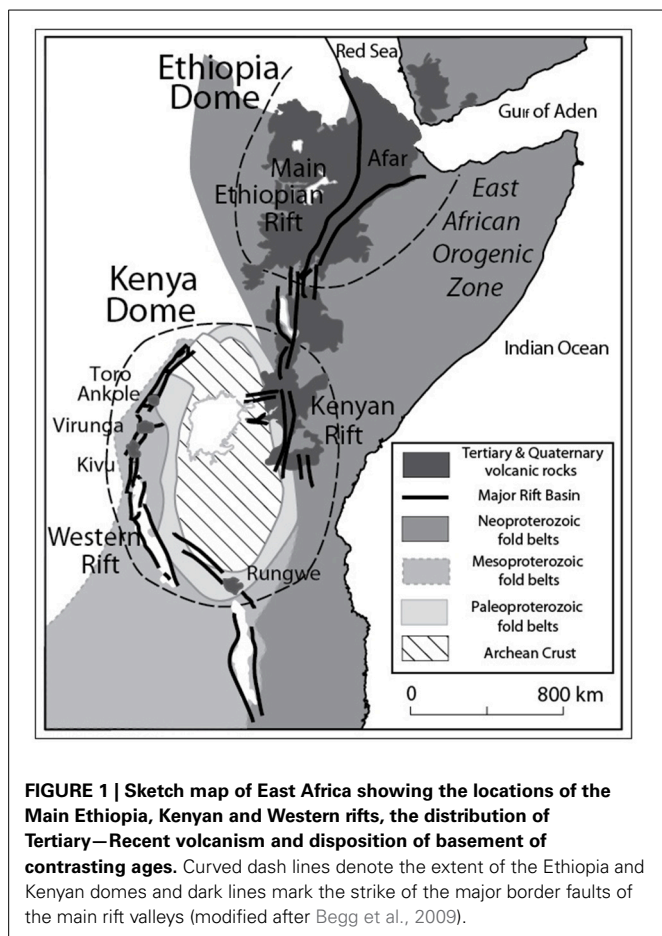
Keywords: Rungwe volcanic province, East African Rift system, African Superplume, high $^3\text{He}/^4\text{He}$ lavas, carbonatite metasomatism, Afar plume, Main Ethiopian Rift, Kenyan Rift

INTRODUCTION

The East African Rift System (EARS)—from southern Tanzania and Lake Malawi, where the African continent begins to break apart, northward to the Afar Triple Junction, where the on-land Danakil Depression meets the oceanic spreading ridges of the Red Sea and Gulf of Aden (**Figure 1**)—provides exceptional opportunities to study geologic processes controlling continental rifting and eventual ocean formation. An outstanding feature of the EARS is the diverse and extensive magmatism associated with the various facets of rifting along its strike, making it a prime target to study the role of magmatism in continental break-up, one of the major issues regarding ocean formation. Results of investigations on this topic thus far suggest that mantle plume-type melting provides the bulk of magmas associated with rifting in the EARS, suggesting active, in this case plume, magmatism plays a significant role in ocean formation (e.g., Rogers, 2006; Furman, 2007).

However, the number and nature of plumes involved in rifting in the EARS are controversial. From the geophysics viewpoint,

only one plume or several plume heads from a single megaplume, the African Superplume, is/are involved (e.g., Ebinger and Sleep, 1998; Nyblade, 2011; Hansen et al., 2012). Geochemical and petrological variations along the length and breadth of the EARS, on the other hand, suggest the possible presence of a number of plumes (**Figure 1**). Although it is widely accepted that the high $^3\text{He}/^4\text{He}$ Afar plume—henceforth termed “C”—centered at Lake Abhe in the Afar region, is present beneath the Main Ethiopian Rift (MER; e.g., Pik et al., 2006; Rooney et al., 2012), it has also been suggested that a Kenyan plume, henceforth termed “K,” exists beneath the Kenyan Rift to the east of Kenyan Dome (e.g., Rogers et al., 2000; Rogers, 2006). Moreover, Chakrabarti et al. (2009) propose a heterogeneous mantle plume supplying the Virunga Volcanic Province (VVP) in the Western Rift. Lavas from Nyiragongo volcano have Nd-Sr-Pb isotopic compositions that overlap with bulk earth values whereas those from Nyiramugira and other VVP volcanoes are more akin to enriched mantle (EMII); we term these plume components “V” and “EMII,” respectively. Finally, a plume compositionally similar



to the “HIMU” plume observed in some ocean islands (where HIMU = high μ or high U/Pb) is proposed for the EARS mantle south of the Turkana Depression in northern Kenya (Furman et al., 2006; Furman, 2007).

The recently-reported high $^3\text{He}/^4\text{He}$ ratios similar to those of the Afar plume at the Rungwe Volcanic Province (RVP) in southern Tanzania extends the influence of mantle plume magmatism to near the southernmost tip of the EARS (Hilton et al., 2011). In this contribution, we present the trace element and Sr-Nd-Pb isotope composition of the RVP samples previously analyzed for $^3\text{He}/^4\text{He}$ ratios (Hilton et al., 2011), first to constrain the nature of the mantle plume source near the site of rift initiation in the southern EARS, and second to compare and contrast such a source with those postulated along the relatively more developed rifts to the north. Our results suggest that the regionally extensive African Superplume with a limited range of composition provides a common source for all reported plume occurrences and, thus, we propose a unified mantle plume model for the entire EARS. The Superplume is best manifested, though still not in pure form, in high $^3\text{He}/^4\text{He}$ magmatism in the MER and RVP as well as in the VVP. In areas where plume magmatism is not obvious geochemically (e.g., absence of high $^3\text{He}/^4\text{He}$ ratio), its influence is otherwise clearly expressed through carbonatite metasomatism. Such a unified model indicates that mantle geodynamics play a crucial role in the initiation

and evolution of the EARS as well as in ocean formation as a whole.

BRIEF GEOLOGIC BACKGROUND

EAST AFRICAN RIFT SYSTEM

The EARS stretches for >2000 km, originating from the Afar triple junction and traversing the Ethiopia Dome southward along the MER before bifurcating to the east and west of the Tanzania Craton of the Kenyan Dome along the Kenyan and Western rifts (Figure 1). The two highlands, the Ethiopia and Kenyan domes, are viewed as geophysical manifestations of upwelling mantle plumes, possibly originating at the core-mantle boundary (e.g., Nyblade et al., 2000; Nyblade, 2011; Hansen et al., 2012). Rift initiation began in southern Ethiopia at approximately 45 Ma (George et al., 1998), with the start of volcanism occurring in northern Ethiopia and Yemen at approximately 30 Ma (Hofmann et al., 1997). Currently, volcanism characterizes the entire length of the EARS, which, together with the Afar Depression, represents one of the largest active continental igneous provinces on Earth (e.g., Bastow et al., 2008).

The geochemistry of recent EARS lavas magmas exhibits strong regional trends with mainly tholeiitic-transitional magmas sourced from the sublithospheric (asthenosphere plus plume) mantle effusing in the Afar region, MER and Kenyan Rift, although the latter region has also been influenced by lithospheric components (e.g., Rogers et al., 1992, 1998, 2000; Furman and Graham, 1999; Furman et al., 2006; Rogers, 2006; Furman, 2007; Chakrabarti et al., 2009; Rosenthal et al., 2009; Rooney et al., 2012). In comparison, volcanism along the Western Rift, which includes the Toro Ankole, Virunga, Kivu, and Rungwe volcanic provinces (Figure 1), started ~later (≤ 23 Ma), is more sporadic and lesser in volume. Although detailed studies have revealed significant geochemical differences among volcanoes within a single province, Western Rift lavas as a whole are silica-undersaturated and include ultrapotassic, hypersodic, and carbonatitic compositions; these are remarkably enriched in incompatible trace and volatile elements (see also, Rogers et al., 1992, 1998; Rudnick et al., 1993; Foley et al., 2012). The strong geochemical enrichment of Western Rift lavas bears the imprint of a continental lithospheric source as well as traces of crustal assimilation in the more differentiated lavas. In general, the range of geochemistry of the Western Rift basalts and their differentiates may have resulted from variable degrees of partial melting due to differences in e.g., depth or pressure, of an underlying, common lithospheric mantle that had been metasomatized by carbonatite-rich fluid (see also, Vollmer and Norry, 1983a,b; Rudnick et al., 1993; Rosenthal et al., 2009; Foley et al., 2012).

RUNGWE VOLCANIC PROVINCE

The post-Miocene mafic lavas in the RVP, which lies at the southernmost extreme of the Western Rift (Figure 1), have been studied in detail by Furman (1995; see also, Furman and Graham, 1999). These include alkali basalts, basanites, nephelinites, and picrites. Phonolites and trachytes are also present, but tholeiitic, ultrapotassic, and hypersodic compositions are absent (see also Harkin, 1960; Ebinger et al., 1989). Compared to the others in the Western Rift, RVP mafic lavas are among the least

potassic, although they still contain high abundances of incompatible trace elements, the behavior of some of which is highly variable and parallels the range observed in global ocean island basalts (OIB). As in other volcanic provinces in the Western Rift, there are geochemical differences within and among the RVP lava suites. Part of the geochemical variations can be ascribed to varying degrees of fractional crystallization, e.g., within the alkali rock suite, although clearly the lavas cannot be related to a single fractionation event. Some of the geochemical variations are due to variation in the degree of partial melting of the source: major and trace element data suggest that the degree of partial melting decreases from alkali basalt to basanite to nephelinite, although, as a whole, RVP magmas are among those produced by the lowest degrees of melting along the Western Rift. Data also suggest that the alkali basalts and some of the nephelinites were generated at shallower depth (lower pressure) than the basanites and another group of nephelinites, but as a whole, melting most probably occurred at pressures that span the garnet-spinel transition (60 ~ 80 km depth). Incompatible trace element abundances, particularly in nephelinite and basanite samples, suggest that the source is a CO₂-rich peridotite containing metasomatic amphibole and phlogopite plus accessory phases ilmenite, apatite and zircon. Significantly, RVP lavas have a relatively restricted range of Sr and Nd isotopes (range presented, but actual data not reported by Furman and Graham, 1999) that fall ~close to the bulk silicate Earth (BSE) value despite the relatively large variations in their major and trace element contents. Carbonatite metasomatism of the continental lithospheric mantle, as opposed to arrival of a mantle plume, has been proposed as the main process that shaped the magma source of RVP lavas (e.g., see also, Furman, 2007).

ANALYTICAL PROCEDURE

We analyzed selected RVP samples for the trace element ($n = 20$) and Sr, Nd and Pb isotopic ($n = 15$) composition from samples previously analyzed for helium isotopic and major element compositions (Hilton et al., 2011). Aliquots of the powders used for major element analysis (Hilton et al., 2011) were analyzed to avoid analytical bias. The sample preparation procedure used is similar to that described in Janney and Castillo (1997). For trace element analysis, about 25-mg powder of each sample was digested with a double-distilled, 2:1 mixture of concentrated HF:HNO₃ acid in a clean Teflon beaker. The digested sample was diluted ~4000-fold with a 1% HNO₃ solution containing 1 ppb ¹¹⁵In as internal standard. Trace element concentrations were obtained using a Finnigan Element 2 high-resolution inductively-coupled mass spectrometer (ICP-MS) at SIO. Calibration was performed using a series of 4 synthetic multi-element standard solutions. Time- and mass-dependent instrumental drift was corrected for by applying a mass-interpolated internal standard correction and by correcting measured sample concentrations with a well-characterized in-house basalt standard analyzed between every 7 samples. Replicate analyses of international rock standards treated as unknown samples show trace element accuracy to be <10%, with most of the elements including the rare earth elements (REE) precise to within 5% (see additional notes under Table 1).

Strontium, Nd and Pb isotope ratios were determined using a 9-collector, Micromass Sector 54 thermal ionization mass spectrometer (TIMS) at SIO. The sample preparation procedure is also similar to that described in Tian et al. (2008). Rock powders were digested using the same procedure described above for trace element analysis. Lead was first separated by re-dissolving the dried samples in 1N HBr and then passing the solutions through a small ion exchange column in a HBr medium. Strontium and REE were separated from the residual solutions in an ion exchange column using HCl as the eluent. Finally, Nd was separated from the rest of the REE in an ion exchange column using alpha hydroxyisobutyric acid as the eluent. Total procedural blanks are <35 pg for Sr, <80 pg for Nd, and <90 pg for Pb.

Strontium isotopic ratios were fractionation-corrected to ⁸⁶Sr/⁸⁸Sr = 0.1194 and are reported relative to ⁸⁷Sr/⁸⁶Sr = 0.710257 for NBS 987. Neodymium isotopic ratios were measured in oxide form, fractionation corrected to ¹⁴⁶NdO/¹⁴⁴NdO = 0.72225 (¹⁴⁶Nd/¹⁴⁴Nd = 0.7219) and are reported relative to ¹⁴³Nd/¹⁴⁴Nd = 0.511857 for the La Jolla Nd Standard. Lead isotopic ratios were measured using a ²⁰⁷Pb–²⁰⁴Pb double spike. Each sample was measured twice as spiked and unspiked aliquots and the fractionation corrected Pb isotopic ratios were derived following the calculations described in Thirlwall (2000). Analytical uncertainty based on repeated measurements of standards is ±0.000018 for ⁸⁷Sr/⁸⁶Sr, ±0.000016 for ¹⁴³Nd/¹⁴⁴Nd, ≤ ±0.003 for ²⁰⁶Pb/²⁰⁴Pb and ²⁰⁷Pb/²⁰⁴Pb, and ≤ ±0.010 ²⁰⁸Pb/²⁰⁴Pb. Two sigma precisions listed in Table 2 refer to within-run statistics.

RESULTS

New analyses for RVP samples are presented in Tables 1, 2 and plotted in Figures 2–4. The samples analyzed consist mainly of alkalic basalt lavas and basaltic tephra from the two volcanic series in the RVP: Older Extrusives, formed by the earliest eruptions of the Ngozi and Katete central volcanoes at ~7 Ma, and Younger Extrusives formed by activities of the Rungwe, Tukuyu, Kiejo, and Ngozi volcanoes from the mid-Pliocene to present (Harkin, 1960; Ebinger et al., 1989; Furman, 1995). Based on silica and total alkali contents, the majority of our samples are basanites and the remainders are picrobasalts, an alkali basalt and a hawaiite (Figure 2A). Some of the basanites are primitive as they contain high MgO (>19 wt%), Ni (>1100 ppm) and Cr (>600 ppm). Similar to other Rungwe mafic samples (Furman, 1995), the basanites and alkali basalt are neither hypersodic nor ultra-potassic (2.2–4.5 wt% Na₂O; 0.8–2.2 wt% K₂O; 0.3–0.5 K₂O/Na₂O) and, thus, differ from most of Western Rift volcanics.

The first significant feature of our new data is that they basically fall within the range of previously-published trace element and Sr-Nd isotopic compositions (Furman, 1995; Furman and Graham, 1999; note that Furman and Graham presented the Sr-Nd isotopic range, but did not report the actual data for RVP lavas). Combined results show RVP samples have variable trace element contents that, as a whole, are more enriched in highly incompatible trace elements than mid-ocean ridge basalts (MORB) and OIB (Figure 2B). Similar to other Western Rift lavas, RVP samples display steep, subparallel, convex-upward normalized patterns that show relative enrichment in Ba and

Table 1 | Trace element composition of RVP basaltic rocks and tephtras.

Sample	RNG-1	RNG-3	RNG-4	RNG-6	RNG-8	RNG-9	RNG-10	RNG-16	RNG-17	RNG-18
<i>Rb</i>	34.7	33.6	28.9	39.4	33.5	31.9	24.9	36.4	47.6	37.9
<i>Ba</i>	1180	1201	1352	1420	1752	2049	1885	1144	1905	750
Th	5.13	6.66	6.35	12.13	7.04	7.59	8.35	3.89	6.53	5.09
U	1.05	1.38	1.44	2.40	1.41	1.28	1.55	0.76	1.30	0.96
Ta	3.33	5.35	7.21	6.75	4.15	3.81	4.89	2.91	4.87	3.79
Nb	58.6	93.2	92.3	117.6	79.6	74.4	96.6	46.3	80.6	43.3
La	69.0	88.9	90.7	114.4	89.4	88.0	105.7	56.8	81.1	74.6
Ce	132.5	178.3	191.6	210.5	177.3	175.9	202.5	120.6	161.1	151.0
Pb	7.6	6.4	6.6	8.1	7.7	7.0	7.1	4.2	8.8	7.2
Pr	14.74	19.81	21.83	20.02	20.01	19.16	20.49	14.57	17.72	17.37
<i>Sr</i>	1182	1291	1549	1354	1626	1579	1787	1378	1403	891
Nd	57.7	71.2	68.7	63.7	64.4	63.1	58.5	57.9	59.9	53.0
Hf	2.91	3.43	3.31	3.39	2.44	2.30	2.77	2.56	3.27	2.22
Zr	142	206	191	226	133	123	156	113	178	107
Sm	7.62	9.76	10.97	8.41	9.14	8.72	8.26	8.56	9.28	8.69
Eu	2.39	2.87	3.17	2.44	2.70	2.84	2.59	2.73	3.17	2.32
Tb	0.93	1.12	1.44	0.97	1.10	1.17	0.89	1.04	1.05	0.99
Dy	4.93	6.05	6.64	5.12	5.51	5.50	4.55	5.06	5.41	4.96
Er	2.34	2.84	2.90	2.52	2.27	2.15	2.11	2.43	2.42	2.18
Yb	1.70	2.15	2.15	1.79	1.80	1.69	1.49	1.84	1.79	1.61
Y	25.5	32.3	31.9	28.4	23.9	23.2	24.6	25.9	29.8	24.3
Lu	0.23	0.30	0.28	0.25	0.23	0.21	0.21	0.23	0.26	0.22

Sample	RNG-19	RNG-20	TAZ09-2	TAZ09-3	TAZ09-7	TAZ09-11	TAZ09-12	TAZ09-15	TAZ09-16	TAZ09-17
<i>Rb</i>	23.8	33.1	24.0	29.6	47.2	28.5	37.4	18.2	23.0	22.2
<i>Ba</i>	644	1207	622	1091	1506	976	1082	2236	1305	1317
Th	3.55	4.07	3.36	3.43	8.83	3.63	6.25	3.91	4.60	5.20
U	0.65	0.72	0.61	0.66	1.92	0.59	0.95	0.76	0.89	0.95
Ta	2.81	2.85	3.03	2.60	7.32	2.31	4.05	3.64	3.22	3.58
Nb	32.3	46.0	32.8	43.9	119.0	38.7	50.2	65.5	52.8	62.7
La	54.9	62.2	51.9	56.6	112.6	55.6	56.5	84.9	62.6	69.9
Ce	115.0	124.0	106.4	113.0	224.0	107.8	110.7	175.9	128.5	141.0
Pb	3.6	6.4	3.8	6.2	6.8	5.4	5.5	4.5	4.5	4.1
Pr	13.54	14.57	13.08	13.70	23.97	11.45	12.87	20.54	15.45	15.13
<i>Sr</i>	561	1315	667	1316	1591	1093	907	1748	1165	1186
Nd	48.4	48.1	46.8	47.9	77.8	41.6	44.0	63.4	52.9	50.3
Hf	2.11	2.71	2.07	2.60	4.10	2.35	3.38	2.63	2.57	2.76
Zr	92	125	92	119	261	103	178	147	123	143
Sm	7.21	7.84	7.05	7.63	11.37	5.83	7.31	10.44	8.71	7.86
Eu	1.93	2.51	1.80	2.36	3.29	1.76	2.26	3.47	2.82	2.42
Tb	0.81	0.93	0.78	0.90	1.46	0.64	0.90	1.32	1.06	0.85
Dy	4.46	4.95	4.21	5.10	6.97	3.88	4.86	6.43	5.47	4.79
Er	1.95	2.31	1.88	2.29	2.96	1.93	2.55	2.93	2.57	2.37
Yb	1.49	1.77	1.44	1.79	2.29	1.33	1.97	2.17	1.87	1.60
Y	20.9	25.5	20.6	24.5	32.9	22.0	26.9	32.3	27.4	27.7
Lu	0.19	0.23	0.19	0.22	0.30	0.19	0.26	0.29	0.24	0.22

Rubidium, Ba and Sr (in italics) were previously analyzed by XRF methods (Hilton et al., 2011). All others were analyzed using a Thermo Finnigan Element 2 high-resolution ICP-MS.

Table 2 | Strontium, Nd and Pb isotopic composition of RVP basaltic rocks and tephtras.

Sample	³ He/ ⁴ He	⁸⁷ Sr/ ⁸⁶ Sr	¹⁴³ Nd/ ¹⁴⁴ Nd	²⁰⁶ Pb/ ²⁰⁴ Pb	²⁰⁷ Pb/ ²⁰⁴ Pb	²⁰⁸ Pb/ ²⁰⁴ Pb
RNG-1	<i>9.19</i>	0.705746	0.512453	18.781	15.614	39.523
RNG-2	<i>6.89</i>	0.704873	0.512619	18.686	15.587	39.057
RNG-3	<i>8.88</i>	0.704603	0.512597	18.503	15.592	39.028
RNG-8	<i>8.62</i>	0.704780	0.512505	18.108	15.562	38.748
RNG-12	<i>10.08</i>	0.704969	0.512460	18.397	15.601	39.006
RNG-16	<i>8.86</i>	0.704926	0.512577	18.222	15.551	38.974
RNG-17	<i>10.31</i>	0.705381	0.512489	18.505	15.601	39.376
RNG-18	<i>14.9</i>	0.705184	0.512470	19.798	15.716	40.183
RNG-19	<i>14.74</i>	0.705561	0.512447	19.867	15.743	40.372
TAZ09-2	<i>14.78</i>	0.705587	0.512447	19.844	15.729	40.347
(duplicate)				19.844	15.728	40.342
TAZ09-7	<i>9.65</i>	0.704651	0.512602	18.384	15.601	39.028
TAZ09-11	<i>12.17</i>	0.705473	0.512426	19.036	15.647	39.658
TAZ09-12	<i>8.69</i>	0.706920	0.512417	17.742	15.563	39.954
TAZ09-13	<i>10.73</i>	0.704626	0.512618	17.978	15.545	39.307
TAZ09-17	<i>10.28</i>	0.704747	0.512574	18.202	15.566	38.971

Ratios of ³He/⁴He (in italics) were previously reported in Hilton et al. (2011). Lead isotopic ratios were analyzed using the double-spike method to correct for mass fractionation during analyses; separate measurements of spiked and unspiked samples were made on different aliquots from the same dissolution. The SBL-74 ²⁰⁷Pb–²⁰⁴Pb double-spike from the University of Southampton was used. Duplicate runs on TAZ09-12 were made on two different sample dissolutions. During this study, the method produced the following results for NBS 981 (n = 11): ²⁰⁶Pb/²⁰⁴Pb = 16.930 ± 0.002, ²⁰⁷Pb/²⁰⁴Pb = 15.4896 ± 0.0027 and ²⁰⁸Pb/²⁰⁴Pb = 36.6999 ± 0.0086. 2σ precisions for individual runs are better than these.

depletion in Rb and Pb (see also Furman and Graham, 1999). They also have higher incompatible trace element contents and normalized highly- to moderately-incompatible trace element ratios such as Ba/Zr, Rb/Sr, and Nb/La than MER lavas. Although Rungwe samples have elevated REE relative to high field strength elements (HFSE) of similar compatibility (e.g., Hf, Zr, Ti, Y), these are not enriched in REE relative to Nb and Ta, unlike the alkalic lavas of Karisimbi volcano or the Italian Province (Furman, 1995). Moreover, most of their incompatible trace elements do not correlate with MgO (not shown). However, their compatible trace elements correlate with MgO and some of their incompatible trace elements correlate with La (Figure 4; see also Furman, 1995).

Samples from RVP plot to the higher ⁸⁷Sr/⁸⁶Sr though lower ¹⁴³Nd/¹⁴⁴Nd side of the BSE values (Figure 3A). They have relatively higher ⁸⁷Sr/⁸⁶Sr and lower ¹⁴³Nd/¹⁴⁴Nd than (a) the majority of MER samples which contain the signature of the proposed Afar plume C (Rooney et al., 2012), (b) the proposed Kenyan plume K (Rogers et al., 2000), and (c) the characteristics of the classic HIMU islands of Saint Helena, Mangaia and Tubuai (Figure 3A). Samples from the Toro–Ankole Province (Davies and Lloyd, 1989) plot exactly within the RVP field and are not shown for clarity of presentation. Moreover, RVP has ⁸⁷Sr/⁸⁶Sr and ¹⁴³Nd/¹⁴⁴Nd ratios that cluster within a limited field bridging the gap between the young, strongly alkaline Nyiragongo volcano, which is proposed to represent the expression in the VVP of mantle plume component V, on the one hand, and Nyiramugira and other VVP lavas representing component EMII, on the other (Chakrabarti et al., 2009). Notably, the latter group of lavas, some

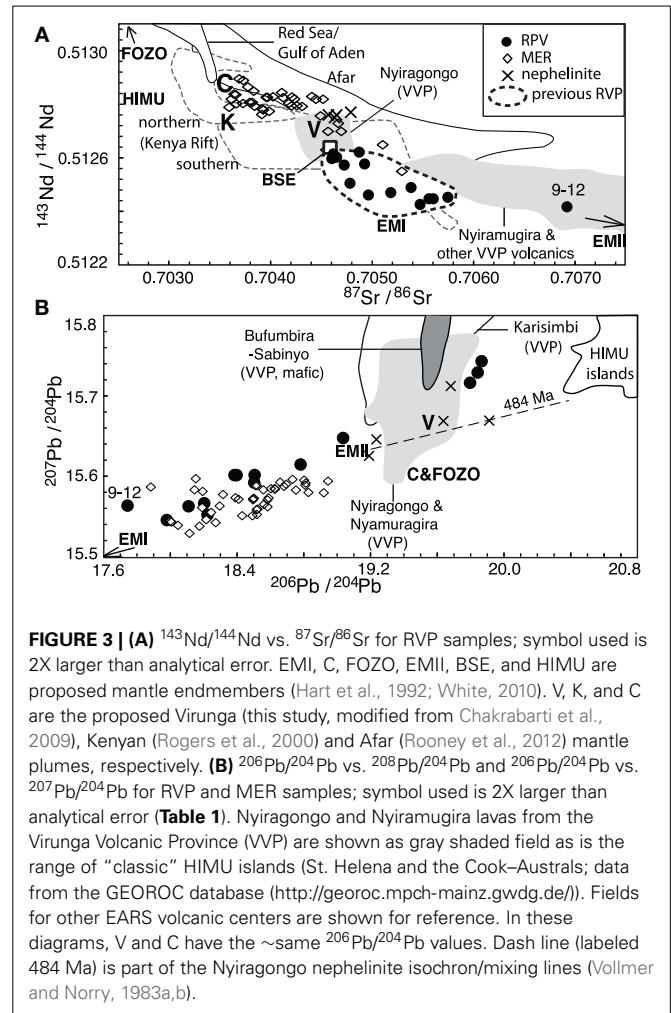
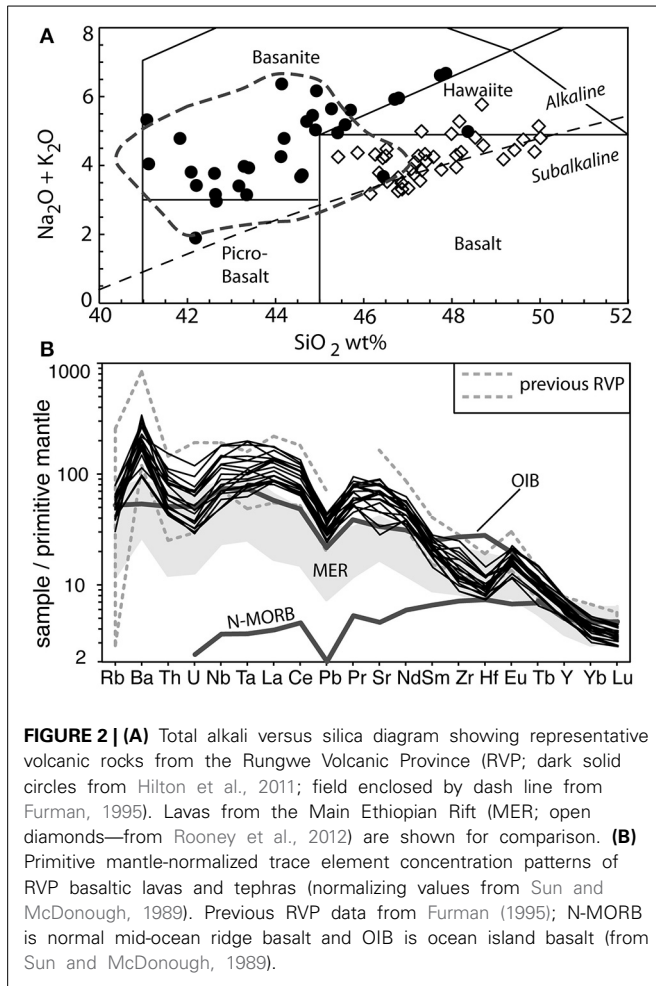
of which possess extremely radiogenic ⁸⁷Sr/⁸⁶Sr ratios, have also been interpreted as products of direct melting of the thick continental lithosphere (Davies and Lloyd, 1989; Lloyd et al., 1991; Furman, 1995, 2007 and references therein; Rogers et al., 1992, 1998; Furman and Graham, 1999).

Finally, RVP has variable Pb isotope ratios that clearly overlap in ²⁰⁶Pb/²⁰⁴Pb with the MER (Rooney et al., 2012) at the depleted (low ²⁰⁶Pb/²⁰⁴Pb) extreme and VVP at the radiogenic (high ²⁰⁶Pb/²⁰⁴Pb) end (Figure 3B). Significantly, the radiogenic Pb RVP samples overlap with the Nyiragongo melilite-bearing nephelinites, some of which have unusually ultra-radiogenic Pb isotopic ratios (e.g., ²⁰⁶Pb/²⁰⁴Pb = 23–62, not shown for clarity; Vollmer and Norry, 1983a,b). A clear exception to this general trend is sample TAZ09–12, which has low ²⁰⁶Pb/²⁰⁴Pb but unusually high ²⁰⁸Pb/²⁰⁴Pb (and ²⁰⁷Pb/²⁰⁴Pb); it also has the highest ⁸⁷Sr/⁸⁶Sr and ~lowest ¹⁴³Nd/¹⁴⁴Nd ratios of the entire RVP sample suite (Figure 3A).

DISCUSSION

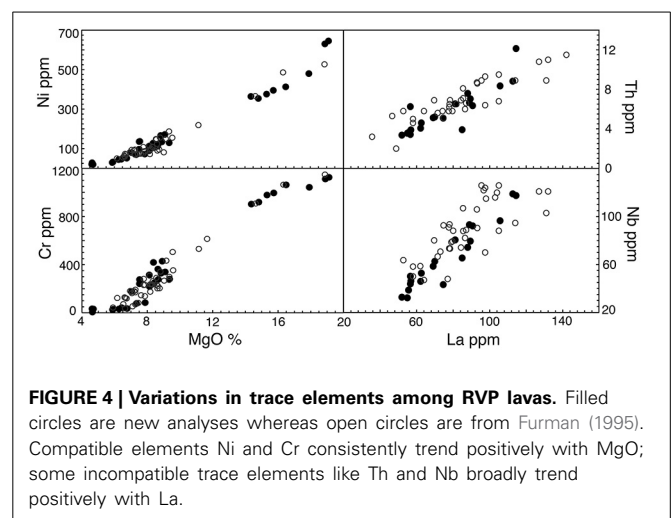
PETROGENESIS OF THE RVP MAGMAS

As a subset of the RVP sample suite (Figures 2–4), the geochemical characteristics of our new analyses are similar to those of other RVP samples. For example, their gross compositional variabilities (e.g., decrease in MgO, increase in SiO₂—Figure 2) are broadly consistent with the effects of varying degrees of fractional crystallization (Furman, 1995). However, the basanites are not petrogenetically linked by a single fractionation event or process as these were erupted at different times and from separate volcanic centers. More importantly, all samples

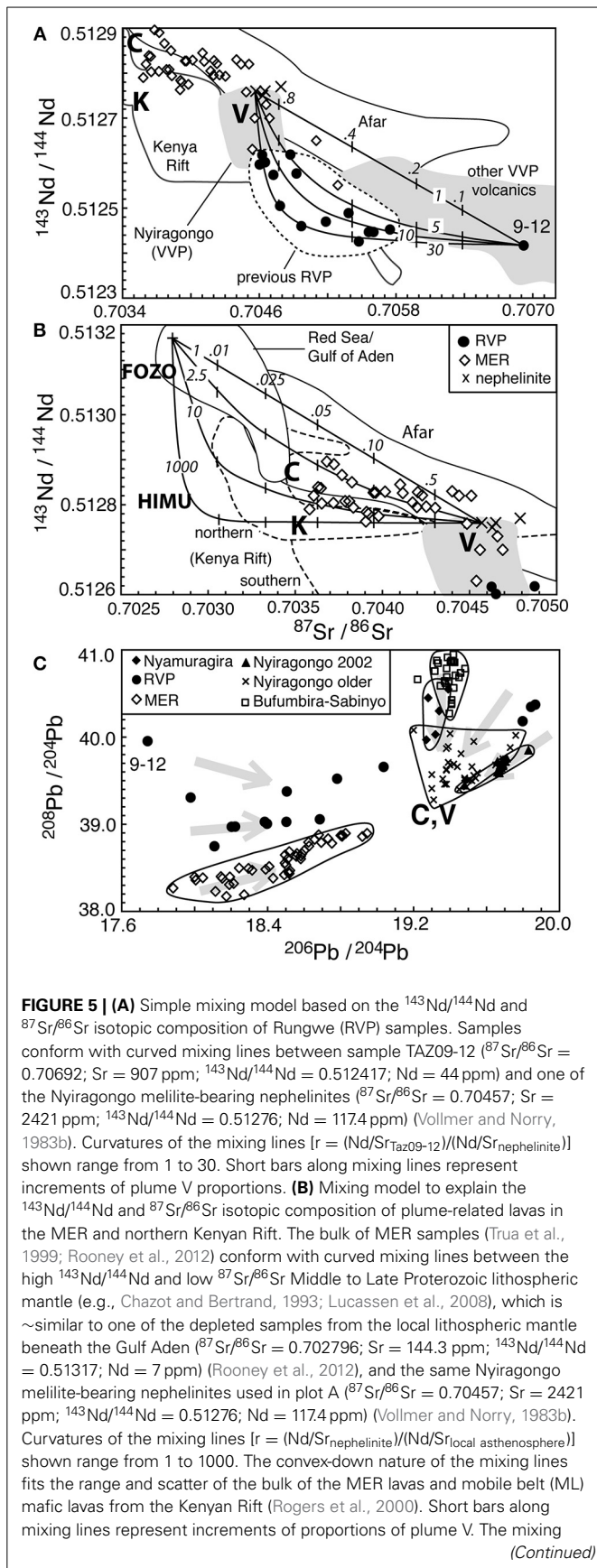


have a range of Sr, Nd, and Pb isotopic ratios (Figure 3), suggesting that, like the rest of RVP samples, they did not come from a single, compositionally homogeneous source. It is also noteworthy that it has been suggested that the overall chemical and Sr and Nd isotopic characteristics of the RVP lavas indicate their parental magmas most probably formed through variable degrees (and pressures) of partial melting of the lithospheric mantle that had been metasomatized by carbonatitic magma (Furman, 1995, 2007; Furman and Graham, 1999).

Closer inspection of the Sr-Nd isotope characteristics (Figure 5A) reveals that RVP samples fall along curved trajectories formed through binary mixing between sample TAZ09-12, which falls within the ~middle of the field for Early Proterozoic lithospheric mantle (see Figure 3A), and one of the melilite-bearing nephelinites from Nyiragongo volcano in the VVP (Vollmer and Norry, 1983a,b). This nephelinite is simply representative of mantle plume V that underlies the VVP; its composition will be discussed in more detail below and in Section RVP in Relation to EARS Magmatism. The convex-down nature of the mixing trajectories is consistent with a lower Nd/Sr ratio in the V endmember compared to the lithospheric mantle endmember. Variation in the curvatures (r-factor) of the mixing lines, between



5 and 30, fits the range and scatter of RVP data. Finally, we note that the proportion of the two endmembers in any given sample is highly variable, lying between ~10–70% lithospheric mantle contributions.

**FIGURE 5 | Continued**

lines also cover some of the mafic lavas from the southern Kenyan Rift, from reactivated craton margin (RCM) and Tanzanian craton (TC) sections (Rogers et al., 2000), but these also contain SCLM component and so are more heterogeneous (see text). It is important to note that the curvatures of some of the mixing lines in plot B requires a factor of 1000 variation in the Sr/Nd ratio and is not observed in the Samples. A more likely explanation for the scatter in the original data is heterogeneity in both end-members, which is certainly expected. **(C)** $^{206}\text{Pb}/^{204}\text{Pb}$ versus $^{208}\text{Pb}/^{204}\text{Pb}$ for RVP, MER and Virunga Volcanic Province. Solid gray arrows represent the general convergence of samples to a narrow range of values—C or V. See Vollmer and Norry (1983a,b) and text for more explanation.

Lead isotope ratios provide more details on the composition of mantle plume V because the low concentration of Pb relative to other elements (Figure 2B) makes them highly sensitive to the effects of radiogenic in-growth and contamination. Vollmer and Norry (1983a,b) proposed that the aforementioned Nyiragongo nephelinites with ultra-radiogenic Pb were formed by carbonatite-rich metasomatizing fluids that permeated the mantle domain beneath the VVP. Notably, Vollmer and Norry also pointed out that the fluids have present-day $^{87}\text{Sr}/^{86}\text{Sr} \sim 0.7046$ and $^{143}\text{Nd}/^{144}\text{Nd} \sim 0.5128$ ratios—values which are within the range of values for the young Nyiragongo and Nyiramugira volcanics that originated from mantle plume V (Figures 3A, 5A). Moreover, these fluids have exceptionally high Th/Pb and U/Pb ratios that produced the ultra-radiogenic Pb isotopic ratios ($^{206}\text{Pb}/^{204}\text{Pb} = 23\text{--}62$) in a number of nephelinites. The high Pb isotope ratio nephelinites define a 484 ± 28 Ma isochron (Vollmer and Norry, 1983a,b), with most of the remaining nephelinites falling along this line (Figure 3B). The same metasomatic fluids also contaminated mantle domains beneath nearby Sabinyo and Bufumbira volcanoes, also in the VVP, producing mafic lavas with unusually homogeneous $^{206}\text{Pb}/^{204}\text{Pb}$ but variable $^{208}\text{Pb}/^{204}\text{Pb}$ and $^{207}\text{Pb}/^{204}\text{Pb}$ ratios. The intersection of the Sabinyo/Bufumbira trends and the nephelinite isochrons in Pb isotope space (Figures 3B, 5C) was interpreted as the original Pb isotopic composition ($^{206}\text{Pb}/^{204}\text{Pb} \sim 19.4$) of the metasomatizing fluids. Significantly, all recently available Pb isotopic data for VVP (Chakrabarti et al., 2009) also trend to the same narrow range of $^{206}\text{Pb}/^{204}\text{Pb}$ values (Figures 3B, 5C). Specifically, the aforementioned Nyiragongo and Nyiramugira lavas, especially the samples erupted in 2002, show a narrow range in $^{206}\text{Pb}/^{204}\text{Pb}$ but broad ranges in both $^{207}\text{Pb}/^{204}\text{Pb}$ and $^{208}\text{Pb}/^{204}\text{Pb}$ ratios. These create vertical to subvertical arrays that trend to $^{206}\text{Pb}/^{204}\text{Pb} \sim 19.3\text{--}19.5$ in Pb-Pb isotopic plots (Figure 5C; see also Chakrabarti et al., 2009).

Taking the Sr-Nd-Pb isotope evidence together, we propose that the mantle plume V beneath VVP, which has a distinct through limited range of isotopic composition (average $^{87}\text{Sr}/^{86}\text{Sr} \sim 0.7045$; $^{143}\text{Nd}/^{144}\text{Nd} \sim 0.5127$; $^{206}\text{Pb}/^{204}\text{Pb} \sim 19.4$; Figures 3, 5), likewise best represents the same mantle plume mainly responsible for the petrogenesis of RVP lavas. We argue that the previously proposed carbonatitic materials that had more or less almost completely metasomatized the lithospheric mantle beneath the VVP for at least, ~500 m.y. (Vollmer and

Norry, 1983a,b) and possibly as long as 1 b.y. (e.g., Davies and Lloyd, 1989; Rudnick et al., 1993; Furman, 1995, 2007; Furman and Graham, 1999; Rogers, 2006; Rosenthal et al., 2009; Foley et al., 2012) represent mantle plume V (see more discussion in Section Western Rift Magmatism). The same mantle plume has not completely metasomatized the lithospheric mantle beneath RVP and, thus, evidence of mixing between mantle plume V and the lithosphere is still evident in the RVP Sr, Nd, and Pb isotopic compositions (**Figures 3, 5**).

Below, we show that the compositional characteristics of mantle plume V are also shared by the majority of Western, Ethiopian and Kenyan rift lavas. We propose that this is due to the carbonatitic metasomatism of the lithosphere beneath the entire EARS by a single mantle plume source: the African Superplume (Castillo et al., 2012).

RVP IN RELATION TO EARS MAGMATISM

Western Rift magmatism

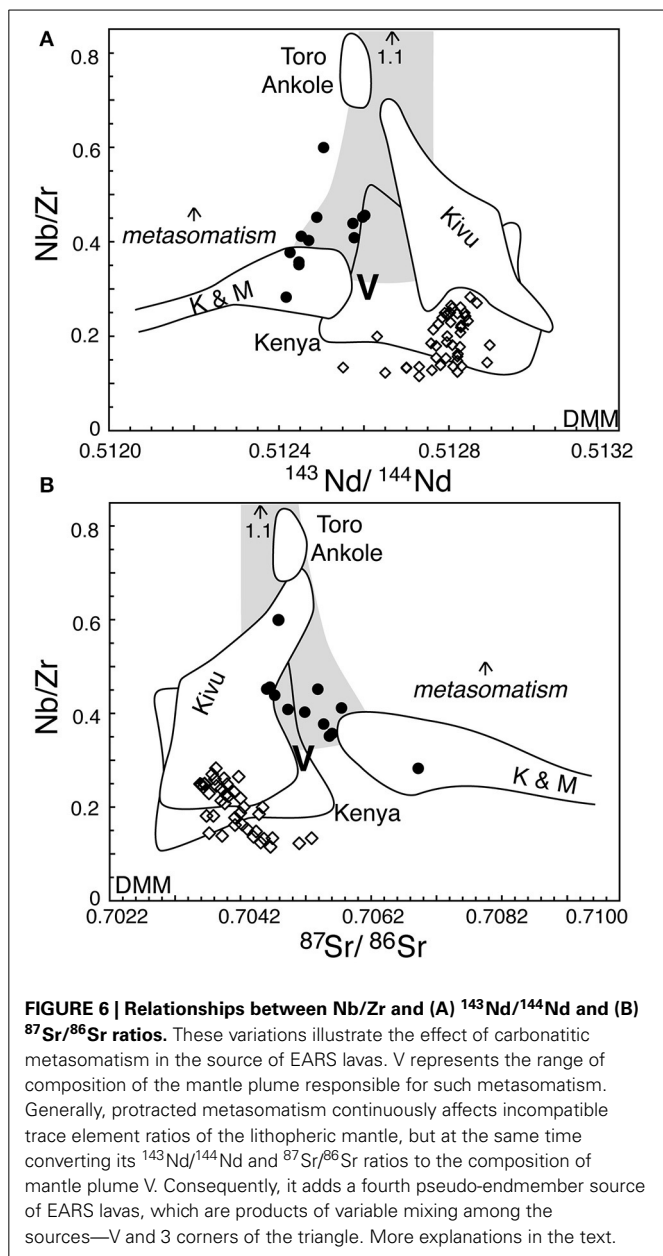
As already noted, there are significant geochemical differences within and among the volcanic provinces along the Western Rift, with some of these differences ascribed to variations in depth and degree of partial melting of the carbonatite-metasomatized continental lithospheric mantle (e.g., Furman, 1995, 2007; Rogers, 2006, and references therein). The differences are indicated, e.g., by the ranges of silica saturation (represented by SiO₂ content) of Western Rift lavas that had been shown to correlate with variations in depth and extent of source melting (see also, e.g., Rosenthal et al., 2009; Foley et al., 2012). For example, undersaturated lavas from RVP together with those from Nyiragongo in VVP and from the Toro–Ankole Volcanic Province indicate lower degrees of melting whereas the silica saturated to mildly undersaturated Kivu Volcanic Province lavas indicate higher degree of melting. The overall geochemistry of the Western Rift lavas likewise indicates slight variation in melting depth from the garnet stability field to the ~shallower depth range of garnet-spinel transition. Geochemical indices such as strong covariation between Al₂O₃ and MgO and steep REE profiles with nearly constant HREE abundances, observed in RVP nephelinites and mafic lavas from Nyiragongo in VVP and from the Toro–Ankole province, are consistent with melting in the presence of residual garnet. On the other hand, RVP alkali basalts and some basanites show a weaker dependence of Al₂O₃ on MgO content and more variable HREE abundances, suggesting that they did not equilibrate with residual garnet (Furman, 2007 and references therein). Finally, some of the geochemical differences in Western Rift lavas, particularly in their trace element contents, may have also resulted from variations in accessory phases (i.e., phlogopite, amphibole, apatite, zircon, ilmenite, sphene) in the local continental lithospheric mantle source beneath each volcano (Furman, 1995).

Despite the aforementioned geochemical differences, and particularly their extreme isotopic variability (**Figures 3A,B**; see also, Rogers, 2006; Furman, 2007), a remarkable feature of Western Rift volcanic provinces is their ⁸⁷Sr/⁸⁶Sr, ¹⁴³Nd/¹⁴⁴Nd, and ²⁰⁶Pb/²⁰⁴Pb ratios converge or trend toward common values, which Furman and Graham (1999) claimed to be ~0.7050, ~0.51264, and ~19.0, respectively. Most of the

Western Rift lavas also have certain trace element ratios, such as La/Nb, Ba/Nb, and Th/Nb, when plotted against ¹⁴³Nd/¹⁴⁴Nd that also converge or trend to a small range of common values. Thus, it is also proposed that the common composition of Western Rift lavas is due to the presence of a “common lithospheric mantle” source beneath the rift, and this was formed due to widespread carbonatitic metasomatism events between 500 and 1000 Ma (Furman and Graham, 1999). Our study concurs that the bulk of Western Rift lavas indeed project to such a common composition, and that their lithospheric mantle source is a product of long-term (up to b.y.) carbonatitic metasomatism (e.g., Vollmer and Norry, 1983a,b; Rudnick et al., 1993; Furman, 1995, 2007; Furman and Graham, 1999; Rogers, 2006; Chakrabarti et al., 2009; Rosenthal et al., 2009; Foley et al., 2012). However, here we argue that such a widely recognized metasomatic effect of carbonatitic material along the EARS is a direct manifestation of mantle plume V (Castillo et al., 2012; see also Rooney et al., 2011).

To illustrate the common trace element composition of the lithosphere, Nb/Zr is plotted against ¹⁴³Nd/¹⁴⁴Nd and ⁸⁷Sr/⁸⁶Sr ratios (**Figures 6A,B**). Both Nb and Zr are high-field strength elements (HFSE) and, hence, they are not susceptible to alteration and cannot be easily fractionated from each other by normal magmatic differentiation processes, but can be modified through metasomatism. **Figures 6A,B** show Western Rift lavas including those from RVP have large variations in all ratios and assume roughly triangular configurations. The Nyiragongo plus Nyiramugira, Muhavura plus Karisimbi volcanoes (all in VVP), particularly their highly differentiated lavas, and Kivu Volcanic Province define the three apices of the triangles. In our proposed model, the ~true composition of mantle plume V is in the interior of the triangles, near the bottom of the Nyiragongo plus Nyiramugira ~vertical trend, the extreme end (i.e., highest Nb/Zr ratios) of which reflects intense metasomatism of the lithosphere by the plume. Indeed, such unusually high ratios of HFSE elements are a diagnostic feature of carbonatite metasomatism (Dupuy et al., 1992; Rudnick et al., 1993; Furman and Graham, 1999; Chakrabarti et al., 2009). We further argue that the ⁸⁷Sr/⁸⁶Sr, ¹⁴³Nd/¹⁴⁴Nd, and ²⁰⁶Pb/²⁰⁴Pb composition of such a common source is best represented by Nyiragongo and Nyiramugira lavas (Chakrabarti et al., 2009), which we have designated in Section Petrogenesis of the RVP Magmas as mantle plume V. Significantly, the common ⁸⁷Sr/⁸⁶Sr and ¹⁴³Nd/¹⁴⁴Nd composition proposed by Furman and Graham (1999) is within the range of the Nyiragongo and Nyiramugira lavas (**Figures 3, 5**). Note that unlike trace element contents that can be continuously increased by long-term and continuous metasomatism (e.g., Nb/Zr in **Figure 6**), long-term metasomatism can modify the isotopic composition of the lithosphere in two ways: (1) by alteration to match that of plume V through mixing, and (2) through radiogenic in-growth, such as the highly radiogenic isotopic composition of melilite-bearing nephelinites (Vollmer and Norry, 1983a,b) in isolated pockets wherein plume material dominates.

One of the net effects of the continuous addition of plume material would be to move the Sr and Nd isotopic values of the different lithospheric mantles to that of plume V and increase the curvature (or r factor) of the mixing relationship between



Sr and Nd isotopes (Figures 5A,B). Similarly, continuous addition of plume material will contaminate the variable Pb isotopic composition of the lithospheric mantles to the plume Pb isotopic composition (Figure 5C). However, with time, the plume Pb isotopic signature becomes more radiogenic because of the high U/Pb ratio of the carbonatitic material (Castillo, 2013) and the shorter half-lives of the U and Th parent isotopes compared to those of the Rb and Sm parent isotopes. These two factors produce the radiogenic Pb isotopic signal that Furman et al. (2006) termed the ocean island HIMU plume component in the southern EARS. Moreover, such BSE-like Sr and Nd plus radiogenic Pb isotopic composition of plume V fall under the “young HIMU” group of mantle plumes or the redefined, large group of “FOZO” mantle plumes (Castillo, 2013; see Section The Nature of the High $^3\text{He}/^4\text{He}$ Mantle Plume V for Additional Discussion).

Recently, Rooney et al. (2014) argued that the HIMU-like Miocene lavas in Ethiopia, adjacent to the northern part of the EARS, are indeed not due to the presence of a HIMU plume (cf., Furman et al., 2006); instead these are products of the long-term evolution of a lithospheric metasome. Such a model is similar to our proposal except that they suggested that the lithospheric metasome was mainly created by subduction fluids during a Neoproterozoic subduction event associated with the Pan-African orogeny and only partly due to the arrival of a mantle plume that is different from the Afar plume C. Their main arguments were that the $^{206}\text{Pb}/^{204}\text{Pb}$ and $^{207}\text{Pb}/^{204}\text{Pb}$ ratios of the Miocene shield volcano near Gerba Guracha on the western Ethiopian plateau are higher whereas their $^{176}\text{Hf}/^{177}\text{Hf}$ isotopes are lower than those of the MER, which carries the Afar plume signature. Such an increase in Miocene Pb isotopes to a certain extent mimics the radiogenic in-growth of Pb isotopes in the aforementioned VVP nephelinites (Vollmer and Norry, 1983a,b), save for the lower initial Pb isotopic composition of the ~younger lithospheric mantle beneath Ethiopia compared to that beneath VVP (Figure 1). Thus, their model for the origin of the Gerba Guracha Pb isotopic signature is similar to our proposal. It is noteworthy, however, that the HIMU-like Pb isotopic signature is also prevalent in the southern EARS (Furman et al., 2006; Furman, 2007), which was not affected by the Neoproterozoic subduction event associated with the Pan-African orogeny (Figure 1). Regarding Hf isotopes, Rooney et al. claimed that the lithospheric metasome inherited the low Lu/Hf ratio of subduction fluids and this maintains the initial low $^{176}\text{Hf}/^{177}\text{Hf}$ ratio of the plume source in the metasome. Significantly, however, the hallmark geochemical depletion in convergent margin magmas of high field strength elements (HFSE), particularly Nb but also Ti and Hf, clearly suggests HFSE depletion in subduction fluids (Gill, 1981). Indeed, magmas derived from such a lithosphere metasomatized by subduction fluids are depleted in HFSE (e.g., Pearce et al., 1990; Castillo, 2008; Arslan et al., 2013). Consequently, Neoproterozoic subduction fluids would have imparted a high, not low, Lu/Hf ratio in the lithospheric metasome that, in turn, would have increased, instead of maintained, the Gerba Guracha $^{176}\text{Hf}/^{177}\text{Hf}$ ratio. Moreover, the lithospheric metasome clearly has high Nb and other HFSE content (Figures 6A,B) and, thus, we argue that the metasome was created mainly by a mantle plume instead of subduction fluids. Finally, as discussed in Section Ethiopian Rift Magmatism, mantle plume V, with lower $^{143}\text{Nd}/^{144}\text{Nd}$ and $^{176}\text{Hf}/^{177}\text{Hf}$ ratios, ~similar to those of the Miocene Gerba Guracha volcano, better represents the Afar plume than C.

In summary, we argue that the compositional convergence of Western Rift (and indeed the entire EARS—see additional arguments in Sections Ethiopian Rift Magmatism and Kenyan Rift Magmatism) lavas is due to the presence of a common mantle plume V, with a limited range of compositions, that had been continuously metasomatizing the compositionally variable lithosphere beneath the Western Rift for the last 500–1000 m.y. Moreover, the aforementioned differences in depth and pressure conditions that affect the extent of partial melting as well as stability fields of garnet, spinel, and accessory phases, in addition to long-term effect of carbonatitic metasomatism, further add

complexities to the composition of Western Rift lavas (see also, Rogers et al., 1992, 1998; Rosenthal et al., 2009; Foley et al., 2012). For example, in contrast to the conclusion of Chakrabarti et al. (2009) that there are at least two components entrained in the heterogeneous mantle plume beneath the southern EARS, the large geochemical variation observed is most probably due to the influence of the compositionally heterogeneous continental lithosphere. Chakrabarti et al. (2009) claimed that the high $^{87}\text{Sr}/^{86}\text{Sr}$, low $^{143}\text{Nd}/^{144}\text{Nd}$ and high $^{207}\text{Pb}/^{204}\text{Pb}$ and $^{208}\text{Pb}/^{204}\text{Pb}$ for ~given $^{206}\text{Pb}/^{204}\text{Pb}$ ratios of Muhavura and Karisimbi volcanoes in VVP suggest the presence of an additional EMII plume component (**Figure 3B**). However, both volcanoes have previously been documented to be products of continental lithospheric mantle as well as contamination by crustal components (e.g., De Mulder et al., 1986; Furman, 2007). Thus, because the compositional characteristics of EMII are those of continental crust material (Jackson et al., 2007), Muhavura and Karisimbi lavas appear to be derived from an EMII mantle plume although this is unlikely to be the case.

Ethiopian Rift magmatism

Lavas from the northern part of the EARS, along and near the MER, are predominantly transitional tholeiites that plot along the boundary between tholeiitic and alkalic rock series and have relatively simpler and more homogeneous compositions than those from the southern EARS (e.g., Rogers, 2006; Furman, 2007; Rooney et al., 2012, 2014, and references therein). Such compositions appear to reflect the relative homogeneity of the underlying Late Proterozoic basement, which also underlies the northern Kenyan Rift (**Figure 1**). However, Ethiopian Rift lavas also exhibit heterogeneity, but this time reflecting their relatively longer rifting history that includes the eruption of a thick sequence of flood basalts prior to continental break-up. The earliest magmatic activity in eastern Africa occurred at 45–35 Ma in southern Ethiopia and, hence, pre-date extension associated with the Ethiopian Rift and the Afar triple junction by at least 15 my. This activity consisted of eruption of older tholeiitic and younger alkalic lava suites, collectively termed the Amaro basalts, which are both relatively enriched in incompatible elements, particularly the alkalic lavas. It is noteworthy that George and Rogers (2002) claimed the Amaro basalts, particularly its alkalic suite member, are the earliest expression of plume magmatism in the EARS from the mantle plume K, which is compositionally distinct from the Afar plume (Rogers et al., 2000).

The next phase of volcanism in the EARS was the Ethiopian flood (trap) basalt volcanism at 30–29 Ma, and this is widely believed to be due to the impact of a mantle plume head at the base of the lithosphere; hence, it is argued by some (e.g., Furman, 2007) to be the true precursor of modern rift magmatism in east Africa (cf., George and Rogers, 2002). Unlike typical flood basalts elsewhere, most of the Miocene Ethiopian flood basalts are transitional tholeiites and have been ascribed to clinopyroxene removal at high (0.5 GPa) crustal pressures (Pik et al., 1999; George and Rogers, 2002; Rogers, 2006; Furman, 2007; Shinjo et al., 2011). In northwestern Ethiopia and Yemen, the flood basalts can be subdivided into a low-TiO₂ and two types of high-TiO₂ groups (e.g., George et al., 1998). The former group ranges from transitional

tholeiites to tholeiites whereas the latter from transitional tholeiites to alkalic basalts. The subdivision is also shown in their trace element contents; the low-TiO₂ group has a generally flat normalized trace element distribution pattern whereas the high-TiO₂ group has an incompatible trace element-enriched pattern, similar to OIB (Pik et al., 1999).

The flood basalt event was followed by syn-extensional alkali basalt magmatism at 19–11 Ma in southern Ethiopia (e.g., George and Rogers, 2002). The alkali basalts are more enriched in incompatible elements and have even more convex upward, OIB-like patterns than the older, 45–35 Ma lavas from the same region. In other words, the pattern of volcanism in the southwest Ethiopian magmatic province is characterized by episodic volcanism that becomes increasingly silica-undersaturated through time (see also Stewart and Rogers, 1996; Shinjo et al., 2011).

At present, volcanic and magmatic activity in the northern part of east Africa is largely confined to the tectonically active segments of the MER, Afar and the active spreading centers of the Red Sea and the Gulf of Aden (Wolfenden et al., 2004). Within Ethiopia, modern volcanism occurs primarily along the well-defined axis of rifting along the MER and in Afar (Hart et al., 1989; WoldeGabriel et al., 1990; Chernet and Hart, 1999; Furman, 2007) and produces bimodal mafic-differentiated lavas. The mafics consist of transitional tholeiitic to mildly alkalic basalts and the differentiated ones are rhyolites and trachytes. Compared to other Ethiopian lavas, MER lavas are less, though still relatively enriched in incompatible trace elements, although the details of enrichment definitely vary with location and age.

As a whole, recent northern EARS lavas have ~higher $^{143}\text{Nd}/^{144}\text{Nd}$ and lower $^{87}\text{Sr}/^{86}\text{Sr}$ ratios than most lavas from the RVP and other EARS volcanic provinces, plotting to the upper left of bulk Earth and *V*-values (**Figures 3A, 5B**). A widely accepted explanation for the Sr and Nd isotopic signature of Ethiopian Rift is that it is mainly a product of mixing among the depleted asthenospheric mantle, Afar plume and continental lithosphere (e.g., Rogers, 2006; Furman, 2007). The most recent iteration of such a model is that the plume is centered beneath Lake Abhe in the Afar region, and that the MER lavas are products of mixing primarily between the proposed depleted mantle source of MORB (DMM) and mantle plume C (Hanan and Graham, 1996), with $^{87}\text{Sr}/^{86}\text{Sr} = 0.7035$, $^{143}\text{Nd}/^{144}\text{Nd} = 0.51287$ and $^{206}\text{Pb}/^{204}\text{Pb} = 19.5$ (Rooney et al., 2012). The Afar plume has high $^3\text{He}/^4\text{He}$ (>15 R_A) ratio (Marty et al., 1996; Scarsi and Craig, 1996; Pik et al., 2006; Rooney et al., 2012), which is commonly viewed as a critical indicator of mantle plumes originating from a more primitive or less degassed lower mantle, and one that has experienced long-term isolation from the convecting upper mantle (Courtilot et al., 2003). Indeed, mantle component C, similar to mantle component FOZO (**Figure 3A**), has been recognized to have the highest $^3\text{He}/^4\text{He}$ among OIB globally (Hanan and Graham, 1996; Hilton et al., 1999). Notably, the Afar plume is the same one with $^3\text{He}/^4\text{He}$ ratio (up to ~20 R_A) that Pik et al. (1999) had proposed to be the main source of some of the high-TiO₂ Ethiopian flood basalts. However, Pik et al. (1999) deduced slightly different $^{87}\text{Sr}/^{86}\text{Sr}$ (~0.704) and $^{143}\text{Nd}/^{144}\text{Nd}$ (~0.51295) ratios for the Afar plume from their dataset.

For the following reasons, we propose that mantle plume V also, if not better, represents the composition of the Afar plume: (a) the $^{206}\text{Pb}/^{204}\text{Pb}$ and $^{208}\text{Pb}/^{204}\text{Pb}$ ratios of plume V are similar to that of plume C (Figures 3B, 5C; Vollmer and Norry, 1983a,b; Rooney et al., 2012); (b) correlation arrays of the few high ($\gg 9 R_A$) $^3\text{He}/^4\text{He}$ MER samples (Rooney et al., 2012) and the high $^3\text{He}/^4\text{He}$ RVP samples with incompatible trace element ratios converge to the \sim same mantle plume composition that has not been affected by carbonate metasomatism (Figures 6, 7); and (c) the $^{87}\text{Sr}/^{86}\text{Sr}$ and $^{143}\text{Nd}/^{144}\text{Nd}$ values of the bulk of MER lavas, particularly the few with high $^3\text{He}/^4\text{He}$ ($>9 R_A$) ratios, do not plot between C and DMM (Figure 3A)—inconsistent with the proposal that the source of MER lavas is dominated (mass fraction = 49–80%) by DMM and mantle plume C (10–43%; Rooney et al., 2012). Regarding the last argument, Rooney et al. (2012) claimed that the composition of MER lavas is due to ternary mixing among mantle plume C, DMM and a small amount of continental lithosphere, but because the three endmembers lie along a pseudo-linear array in the Sr against Nd isotope space, then samples lie along a binary mixing trajectory between C and an enriched component created by mixing between DMM and lithosphere. If this is true, then it is very similar to our proposed scenario in which the bulk of MER lavas are binary mixtures between enriched plume V and depleted, Late Proterozoic lithosphere (Figure 5B). In other words, we do not necessarily disagree that there may be three endmembers involved (Figures 5A,B), but the bulk of MER lavas is simply due to binary mixing between Late Proterozoic lithosphere and mantle plume V.

In terms of Pb isotopic compositions, MER lavas are comparatively less radiogenic than those from the Western Rift, with a number of exceptions, e.g., RVP lavas are \sim similar to MER lavas (Figures 3B, 5C). Rooney et al. (2012) propose that the $^{206}\text{Pb}/^{204}\text{Pb}$ ratio of their mantle plume C is ~ 19.5 , which is similar to that of plume V. This is remarkable given the fact that the $^{206}\text{Pb}/^{204}\text{Pb}$ value of plume V is constrained from the intersection of the Pb isotopic analyses from several Western Rift volcanoes (e.g., Vollmer and Norry, 1983a,b; Figure 5C) whereas that of plume C is from the intersection of Pb isotopic analyses from several Ethiopian Rift volcanoes (Rooney et al., 2012). It is also remarkable that in addition to the negative linear relationships of the high $^3\text{He}/^4\text{He}$ and $^{206}\text{Pb}/^{204}\text{Pb}$ samples, there is a strong positive correlation between He and Pb isotopes for RVP and MER lavas with $^3\text{He}/^4\text{He}$ ratios $>9 R_A$ (Figure 8C). Note that a similar (positive) correlation between He and Pb isotopes has been observed along the Reykjanes Ridge with $^3\text{He}/^4\text{He}$ and $^{206}\text{Pb}/^{204}\text{Pb}$ both increasing toward the Icelandic plume (Hilton et al., 2000). However, no correlations exist among He, Sr and Nd isotope systems for either RVP or MER lavas (Figures 8A,B). Such a lack of correlation (often termed “decoupling”) has been noted previously and attributed to either a large He concentration contrast between plume and lithospheric mantle, making He the only tracer not overwhelmed by lithospheric additions, or prior metasomatic enrichment of the lithospheric mantle by plume-derived volatiles (Graham et al., 2009).

Here we propose an additional possibility that the volatiles associated with the arriving plume material beneath the lithospheric mantle make it relatively \sim faster and/or \sim easier to

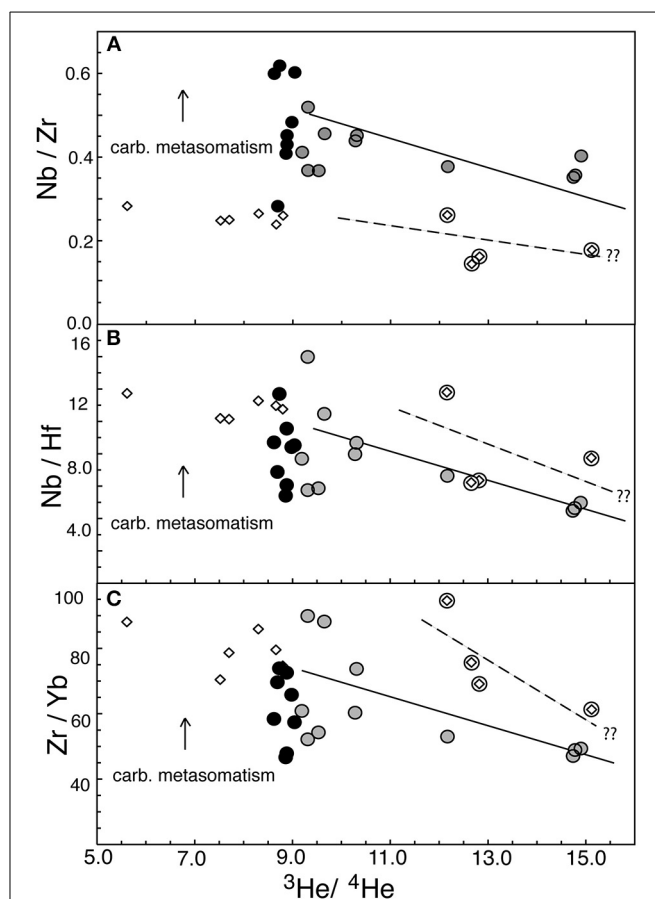
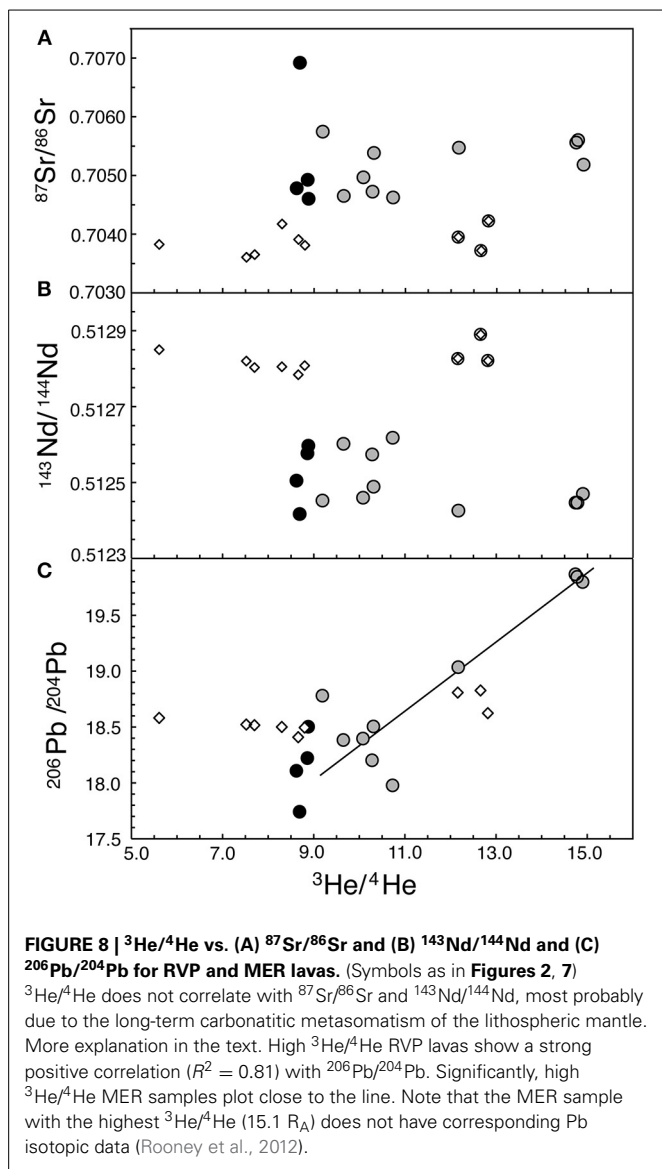


FIGURE 7 | Variations of (A) Nb/Zr, (B) Nb/Hf, and (C) Zr/Yb against $^3\text{He}/^4\text{He}$ for RVP and MER samples. (Symbols as in Figure 2) High $^3\text{He}/^4\text{He}$ ($>9 R_A$)—gray circle for RVP; circled diamond for MER) lavas from RVP and MER appear to merge to \sim common values, which we propose as plume V. The compositional variabilities in the bulk of RVP and MER lavas are due to differences in basement lithologies (see Figure 1) and effect of metasomatism (i.e., compare to Figure 6). That is, plume V that has high Nb content and Zr/Yb ratio than the lithospheric mantle, and continuous addition of the plume material increases the Nb/Zr, Nb/Hf, and Zr/Yb ratios of the metasomatized mantle.

participate in crustal volcanism compared to solid tracers of the plume in special tectonic settings such as in the RVP and along the MER (see Section The Nature of the High $^3\text{He}/^4\text{He}$ Mantle Plume V below). Such a process is due to the “outgassing” of abundant CO_2 from the carbonatitic plume material at depth that then acts as the carrier phase for the trace gases, as is proposed to explain the decoupling of helium from other geochemical tracers in the Hawaiian plume (e.g., Hofmann et al., 2011). This notion is highly consistent with abundant CO_2 outgassing along the EARS (e.g., Craig et al., 1977; Fischer et al., 2009; Barry et al., 2013). In contrast, the solid tracers are first involved in metasomatic reactions with the entire lithospheric mantle prior to actively participating in crustal volcanism. This concept is consistent with the measured plume signature in He, Ne and Ar gases trapped in mafic crystals and xenoliths from the entire EARS (Halldórsson et al., 2014) despite the apparent lack and/or variable presence of such a signature in other geochemical tracers.



Kenyan Rift magmatism

In general, Kenyan Rift lavas are less alkalic and geochemically less enriched than those erupted along the Western Rift although their Sr-Nd-Pb isotope ratios are still broadly similar to OIB values (Rogers, 2006; Furman, 2007; and references therein). In detail, the former is compositionally more diverse than both Ethiopian and Western rifts as its lavas range from tholeiite basalt through alkali basalt to basanite and up to nephelinite (Rogers et al., 2000). Kenyan Rift lavas generally can be divided into two broad groups (Rogers, 2006; Rogers et al., 2000). The first is relatively depleted in Sr, Nd and Pb isotopes ($^{87}\text{Sr}/^{86}\text{Sr} = 0.7030\text{--}0.7035$, $^{143}\text{Nd}/^{144}\text{Nd} = 0.5130\text{--}0.5127$ and $^{206}\text{Pb}/^{204}\text{Pb} = 18.3\text{--}19.8$), defines a steep negative trend on the Nd vs. Sr isotope diagram and plots on an array close to the northern hemisphere reference line (NHRL; Hart, 1988) on conventional Pb isotope diagrams. These isotopic values are claimed to be derived directly from a sublithospheric mantle source (Rogers

et al., 2000). In comparison, the second group is relatively more enriched ($^{143}\text{Nd}/^{144}\text{Nd} = 0.5124\text{--}0.51275$, $^{87}\text{Sr}/^{86}\text{Sr} = 0.7035\text{--}0.7056$ and $^{206}\text{Pb}/^{204}\text{Pb} = 17.6\text{--}21.2$), defines flat-lying arrays on Nd vs. Sr isotope space and has a much greater scatter and spread on Pb isotope diagrams, with many analyses plotting above the NHRL. To a first order, the first group consists of lavas from northern rift segments traversing the Middle to Late Proterozoic Pan-African Mozambique belt whereas the second group generally is found along rift segments close to the Tanzania Craton, through a zone of reactivated craton margin created during the Pan-African orogeny (Rogers et al., 2000; Rogers, 2006; Furman, 2007), which is represented by the East African Orogenic zone in Figure 1. Significantly, the differences in the compositions of parental mafic magmas in the Kenyan Rift generally correlate with differences in age and composition as well as in seismic anisotropy of the underlying lithosphere (Rogers et al., 2000; Rogers, 2006). For example, although the broadly negative correlation between Zr/Nb (<2–7) and Ce/Y (1–8) in Kenyan Rift lavas generally indicates derivation from a garnet-bearing mantle source region as a result of <3% melting, those basalts from that segment of the rift underlain by the Tanzania Craton and, to a certain extent by reactivated craton margin, have higher Ce/Y and lower Zr/Nb ratios than those erupted through the Pan-African basement implying an origin either at greater depth or from a more trace element-enriched source region (Rogers et al., 2000).

Despite these compositional variations, Kenyan Rift lavas are similar to Western Rift lavas as they also converge toward a common composition, although this time with $^{87}\text{Sr}/^{86}\text{Sr} = 0.7030\text{--}0.7035$ and $^{143}\text{Nd}/^{144}\text{Nd} = 0.5130\text{--}0.5127$ according to Rogers and co-workers (Rogers et al., 2000; George and Rogers, 2002; Rogers, 2006). Rogers and co-workers also proposed that such a common composition originates from mantle plume K, which is compositionally distinct from the Afar plume C (Figures 3A, 5B). They also claimed the compositional variation of Kenyan Rift lavas is due to the variable types of continental lithosphere beneath the different segments of the Kenyan Rift that mixed with the Kenyan plume. In other words, the basic principle of the model we propose to explain the compositional variations of Ethiopian and Western Rift had already been advocated by Rogers and co-workers for Kenyan Rift. The only difference between the models is the difference in the composition of the mantle plumes involved. In our proposed model, we argue that mantle plume V is as good if not better than plume K as source of Kenyan Rift lavas (Figure 5B). The spread and scatter of available Sr and Nd isotopic data for the less enriched lava group from the northern Kenyan Rift (i.e., the mobile group of Rogers et al., 2000) fit nicely with the convex down nature of the a binary mixing lines between V and a depleted, Middle to Late Proterozoic Pan-African lithospheric mantle beneath the northern Kenyan Rift, as in our proposed model for the MER (see also Figure 1). As before, the convex-down nature of the mixing trajectories is consistent with a lower Nd/Sr ratio in the Late Proterozoic lithosphere compared to the V endmember. Variation in the curvatures (r-factor) of the mixing lines between 1 and 1000 fits the range and scatter of the bulk of Kenyan Rift data. Finally, we note that the proportions of the two endmembers in any given sample are highly variable, lying between ~1–50% mantle plume V contributions.

The same mixing lines also cover some of the mafic lavas from southern Kenyan Rift, although the bulk of the latter group are products of mixing between V and the heterogeneous continental lithospheric mantle beneath the Early Proterozoic as well as Archaean lithosphere that underlie the southern Kenyan Rift, as in our proposed model for the Western Rift (**Figure 5**). Indeed, some of these enriched Kenyan Rift lavas had been pointed out to converge, together with Western Rift lavas, to the aforementioned “common lithospheric mantle” source (Furman and Graham, 1999). Unfortunately, the Pb isotopic characteristics of the Kenyan Rift, and the entire EARS as a whole, are very heterogeneous and poorly understood (e.g., Furman and Graham, 1999; Furman, 2007). The main reason for this is that the continental lithosphere is more enriched in Pb than the mantle (e.g., Hofmann, 1997) and, thus, is more isotopically heterogeneous. Combined with the shorter half-lives of U and Th compared to Rb and Sm (Section Western Rift Magmatism), all what we can conclude at this point is that most of them converge to $^{206}\text{Pb}/^{204}\text{Pb} \sim 19.4$ (**Figure 5C**). A rigorous test of our model using Pb isotopes is beyond the scope of this study. In any case, it is also noteworthy that the aforementioned Amaro basalts (Section Ethiopian Rift Magmatism) that are claimed by George and Rogers (2002) to be the oldest manifestation of the Kenyan plume also plot along these mixing arrays, consistent with our proposal that the mantle plume signature of the entire EARS can be traced to a single mantle plume regardless of location and time of eruptions (**Figure 5B**).

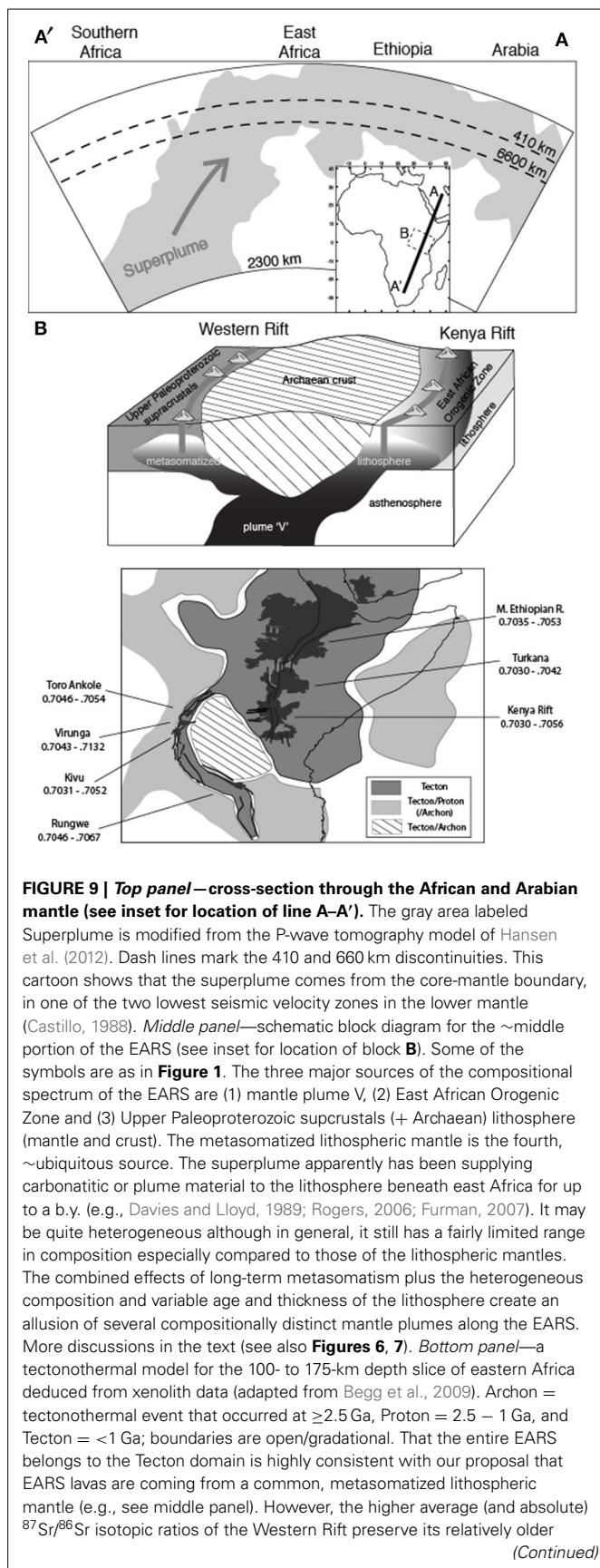
In summary, the ranges in composition of the bulk of lavas from Western, Ethiopian and Kenyan rifts can be modeled as products of mixing between a common, mantle plume V with a limited compositional range and two main types of lithospheric mantles with different ages and compositions. In our proposed model, variable mixtures of Middle to Late Proterozoic lithosphere and plume V produce the compositional array of the less enriched group of northern Kenyan Rift and Ethiopian rift lavas (**Figure 5A**). On the other hand, the compositional array of the more enriched group of southern Kenyan Rift lavas and the bulk of Western Rift lavas is due to variable mixtures of plume V and Early Proterozoic lithospheric as well as Tanzania cratonic mantle and crust (**Figure 5B**). The long-term effects of mantle plume metasomatism of the lithospheric mantle add another layer of variations to the composition of EARS lava, making a simple, straightforward modeling very difficult (**Figure 6**). That is, the bulk lavas from the northern EARS (i.e., along Ethiopian and northern Kenyan rifts) that cut through Middle to Late Proterozoic basement plot along binary mixing lines between plume V and \sim depleted Late Proterozoic lithospheric mantle whereas the bulk lavas (Kivu lavas are clear exceptions) from the Western Rift (**Figure 1**) plot on the different binary mixing arrays, between plume V and the Early Proterozoic and Archaean lithospheric mantle, which for simplicity is represented here by sample TAZ09-2 (**Figures 5A,B**). Some of the EARS lavas are direct products of mixing between the two lithospheres, with the mantle plume V providing the heat (see inset in **Figure 5**).

THE NATURE OF THE HIGH $^3\text{He}/^4\text{He}$ MANTLE PLUME V

Our proposed model calls for a ubiquitous mantle plume V input beneath eastern Africa (**Figure 9**) to explain the genesis of the

bulk of EARS magmas. Furthermore, its long-term metasomatic effect on the lithosphere likewise explains the compelling geochemical evidence for a strong lithospheric overprint in Western Rift and southern Kenyan Rift lavas. One of the major issues that need to be resolved is the survival of high (plume-like) $^3\text{He}/^4\text{He}$ ratios at RVP and MER given the narrow range of $^3\text{He}/^4\text{He}$ ($6 \pm 0.9 R_A$) typical of lithospheric mantle in Tanzania (Hilton et al., 2011) and elsewhere (Gautheron and Moreira, 2002). **Figure 8** shows plots of $^3\text{He}/^4\text{He}$ vs. $^{87}\text{Sr}/^{86}\text{Sr}$, $^{143}\text{Nd}/^{144}\text{Nd}$, and $^{206}\text{Pb}/^{204}\text{Pb}$ for the RVP sample suite and lavas from the MER (Rooney et al., 2012). In the absence of evidence that depleted MORB mantle (DMM) as a contributor to the petrogenesis in the Western Rift (Furman, 2007; but see Rooney et al., 2012 for a difference in opinion), the lack of correlations among He, Sr and Nd isotope systems for either RVP or the MER (**Figure 8**) suggest that the MORB-like $^3\text{He}/^4\text{He}$ values ($8 \pm 1 R_A$) at RVP and MER must therefore result from long-term metasomatic enrichment of the lithospheric mantle by plume-derived volatiles (Graham et al., 2009). As noted earlier (Section Western Rift Magmatism), our model posits that the long-term metasomatic process beneath the EARS will cause the long-lived radiogenic Sr and Nd isotopic compositions of the bulk lithosphere to be near or up to that of mantle plume V; this is true for the majority of localities in the EARS because the isotopic decay of the parent ^{87}Rb and ^{147}Sm nuclides with long half-lives cannot keep up with the continuous supply of plume material with \sim constant isotopic compositions. In contrast, however, plume metasomatism cannot increase the $^3\text{He}/^4\text{He}$ of the bulk of lithosphere up to the distinct, high value (at least up to $\sim 20 R_A$) of plume V because of the presence of abundant metasomatic U and Th, which \sim instantaneously produce radiogenic ^4He because of their much shorter half-lives, constantly reducing the He isotopic composition of the metasomatized lithosphere. Thus, the $8 \pm 1 R_A$ value observed in fluids from volcanic fumaroles and hydrothermal springs in the EARS must be derived from the metasomatized lithospheric mantle, and reflects the delicate balance between mantle plume influx of high $^3\text{He}/^4\text{He}$ from below and the radiogenic He production by U and Th in the metasomatized lithosphere beneath the surface. This notion is consistent with coupled He-Ne isotope systematics of the EARS which are best explained by admixture between a single mantle plume source and either a DMM or SCLM component but not both (Halldórsson et al., 2014), thus highlighting the fact that the all $^3\text{He}/^4\text{He}$ values are not necessarily representative of source features (Hilton et al., 2011).

In contrast, there is a strong positive correlation between He and Pb isotopes for some RVP and MER lavas with $^3\text{He}/^4\text{He}$ ratios $>9 R_A$ (**Figure 8C**). These high $^3\text{He}/^4\text{He}$ and $^{206}\text{Pb}/^{204}\text{Pb}$ samples also appear to converge to negative linear relationships with some refractory trace element ratios toward a distinct mantle source (**Figure 7**). Thus, as in the case of Sr-Nd isotopes (**Figure 3A**), He-Pb (and trace element) arrays reflect mixing of an enriched mantle component with high $^3\text{He}/^4\text{He}$ ($>15 R_A$), $^{206}\text{Pb}/^{204}\text{Pb}$ (19.5) and distinct incompatible trace element ratios with lower $^3\text{He}/^4\text{He}$ ($\sim 6 R_A$), variable $^{206}\text{Pb}/^{204}\text{Pb}$ and lower trace element contents, characteristic of a compositionally heterogeneous continental lithospheric mantle. We point out earlier (Section Ethiopian Rift Magmatism) that a similar (positive) correlation between He and Pb isotopes have been observed along

**FIGURE 9 | Continued**

lithospheric source than that of the eastern rifts. Sources of $^{87}\text{Sr}/^{86}\text{Sr}$ data: Main Ethiopian Rift, Rooney et al. (2012) and Trua et al. (1999); Turkana, Furman et al. (2006); Kenyan Rift, Rogers et al. (2000); Toro–Ankole, Rosenthal et al. (2009); Virunga, Vollmer and Norry (1983b); Rogers et al. (1992); and Chakrabarti et al. (2009); Kivu, Furman and Graham (1999); and Rungwe (this study).

the Reykjanes Ridge with $^3\text{He}/^4\text{He}$ and $^{206}\text{Pb}/^{204}\text{Pb}$ both increasing toward the Icelandic plume (Hilton et al., 2000). In the EARS, we argue that the continuous arrival from below of mantle plume V material for a long time (up to b.y.) metasomatizes the different lithospheric mantles beneath eastern Africa, creating a more or less homogenized lithospheric mantle beneath the region (**Figure 9**). Such a lithospheric mantle is sampled by EARS magmatism, creating a single, ~younger tectonothermal architecture along the entire rift system (Begg et al., 2009), despite differences in the original lithospheric compositions. On the other hand, the unique tectonic and structural settings at both RVP and MER allow some of the material to make it to the surface quicker (<500 m.y.) and, thus, still preserve some of the plume's original (e.g., $^3\text{He}/^4\text{He} > 15 R_A$, $^{206}\text{Pb}/^{204}\text{Pb} > 19$) signature. This material mixes with other components on their way to the surface (**Figures 5, 6**). Specifically, RVP lies in a triple rift junction (**Figure 1**) whereas the MER, like the bulk of the Ethiopian Rift, is the most developed, or has the most extended continental lithosphere, in the EARS (Rooney et al., 2012 and references therein).

In many respects, the African Superplume is the obvious candidate as the ultimate host of our proposed mantle plume V with a high $^3\text{He}/^4\text{He}$ component given its postulated origin in the lowermost mantle and connection with seismically anomalous upper mantle beneath eastern Africa (Castillo, 1988; Nyblade, 2011; Hansen et al., 2012). Our model in principle is similar to a single, heterogeneous mantle plume with a classic HIMU end-member composition (high $^{206}\text{Pb}/^{204}\text{Pb} > 20$) that is proposed to lie beneath the southern EARS only (Furman et al., 2006). However, such a classic HIMU mantle plume most likely has low $^3\text{He}/^4\text{He}$ (<8 R_A) ratio (Class et al., 2005; Castillo, 2013), and fails to account for the Sr, Nd and particularly the Pb isotope characteristics of the RVP dataset (**Figure 3**) and cannot explain the positive correlation between high $^3\text{He}/^4\text{He}$ and Pb isotopes (**Figure 8C**). In our proposed model, the plume V underlying eastern Africa is part of the broad group of young HIMU mantle plumes (e.g., Thirlwall, 1997; Stracke et al., 2005) that has also been designated as the FOZO group of plumes that invariably have high $^3\text{He}/^4\text{He}$, high $^{206}\text{Pb}/^{204}\text{Pb}$ (but still lower than the classic HIMU islands of St. Helena, Mangaia and Tubuai) and near bulk Earth $^{87}\text{Sr}/^{86}\text{Sr}$ and $^{143}\text{Nd}/^{144}\text{Nd}$ composition (Castillo, 2013) and originate directly from the lower mantle (Castillo, 1988).

SUMMARY AND IMPLICATIONS

Our results have a number of profound geologic implications. At the local scale, they lead to a clearer understanding of the petrogenesis of RVP magmas. Volatile-rich (primarily carbonatitic)

plume materials must have metasomatized the Rungwe lithospheric mantle at various times, and raised the $^3\text{He}/^4\text{He}$ ratio from a starting value of $\sim 6 R_A$ up to higher values, and led to the almost complete hybridization of some of its trace element plus Sr, Nd, and, to a large extent, Pb isotope compositions. Some of the compositional variations of RVP lavas are due to variations in depth and pressure of melting of such a metasomatized source plus fractional crystallization. However, some and/or more recently arrived plume materials partially bypass the metasomatism process and produce lavas that still bear some of the plume signature (e.g., high $^{206}\text{Pb}/^{204}\text{Pb}$ and $^3\text{He}/^4\text{He}$ up to 15 R_A).

Regionally, the proposed RVP and plume heads along the EARS can simply be backtracked to a common mantle plume, which most likely originates from the African Superplume. Manifestations of the bulk of EARS volcanism can be explained by mixing between plume V and ambient or local asthenospheric mantle, which was heterogeneous to start with, but is continuously being metasomatized by mantle plume V. Our preferred interpretation, which does not require the presence of several compositionally distinct plumes along the EARS (Figure 9), is that the composition of the Ethiopian and northern Kenyan rift lavas would involve mixing between plume V and the Middle to Late Proterozoic Pan-African lithospheric mantle (e.g., Chazot and Bertrand, 1993; Lucassen et al., 2008), which approaches the composition of depleted samples from the local lithospheric mantle beneath the Gulf of Aden (Rooney et al., 2012). A similar scenario is proposed for the southern Kenyan and Western rift lavas: mixing between V and the more radiogenic mantle of the Early Proterozoic lithosphere plus Tanzania Craton (e.g., Rogers et al., 2000; Rogers, 2006). The northern and southern mixing scenarios in principle are respectively similar to the currently proposed origins of MER (Rooney et al., 2012) and Kenyan (Rogers et al., 2000) rift lavas, except the current model calls for a common mantle plume V. The proposed mixing scenario shares attributes with a common lithospheric mantle model invoked for Western and southern Kenyan Rifts (Furman and Graham, 1999) and a HIMU model for the southern EARS. A good example how a common mantle plume V with a limited compositional variability can produce compositionally heterogeneous lavas that are being interpreted as derived from more than one plume is the VVP. Here, mafic lavas are heterogeneous, particularly in terms of their Pb isotopic composition, because these were erupted through the thick Tanzanian craton and, hence, primarily reflect the heterogeneity of the Tanzania lithosphere (e.g., Rogers et al., 1998; Chakrabarti et al., 2009).

Finally, our proposal that multiple mantle plume heads or conduits with a high $^3\text{He}/^4\text{He}$ composition are directly linked to a large, geophysical feature in the lower mantle (Castillo et al., 2012; Halldórsson et al., 2014) provides additional constraints for the upwelling mechanics of the lower mantle (Castillo, 1988; Montelli et al., 2006). In turn, this could lead to a better understanding of the buoyancy support mechanism of the volatile- and light element-rich mantle plume material impinging the Ethiopia and Kenyan domes and how it relates physically to lithospheric rifting along the EARS.

ACKNOWLEDGMENTS

We acknowledge the Petrology and Geochemistry program of NSF (EAR-1019489) for support, Y. Xu and W. White who provided helpful comments and S. Song for editorial handling.

REFERENCES

- Arslan, M., Temizel, Y., Abdioğlu, E., Kolaylı, H., Yücel, C., Boztuğ, D., et al. (2013). ^{40}Ar - ^{39}Ar dating, whole-rock and Sr-Nd-Pb isotope geochemistry of post-collisional Eocene volcanics in the southern part of the Eastern Pontides (NE Turkey): implications for magma evolution in extension-induced origin. *Contrib. Mineral. Petrol.* 166, 113–142. doi: 10.1007/s00410-013-0868-3
- Barry, P. H., Hilton, D. R., Fischer, T. P., de Moor, J. M., and Mangasini, F. (2013). Helium and carbon isotope systematics of cold “mazuku” CO_2 vents and hydrothermal gases and fluids from Rungwe volcanic province, southern Tanzania. *Chem. Geol.* 339, 141–156. doi: 10.1016/j.chemgeo.2012.07.003
- Bastow, I., Nyblade, A., Stuart, G., Rooney, T., and Benoit, M. (2008). Upper mantle seismic structure beneath the Ethiopian hot spot: rifting at the edge of the African low-velocity anomaly. *Geochem. Geophys. Geosyst.* 9:Q12022. doi: 10.1029/2008GC002107
- Begg, G. C., Griffin, W. L., Natapov, L. M., O'Reilly, S. Y., Grand, S. P., O'Neill, C. J., et al. (2009). The lithospheric architecture of Africa: seismic tomography, mantle petrology, and tectonic evolution. *Geosphere* 5, 23–50. doi: 10.1130/GES00179.1
- Castillo, P. R. (1988). The Dupal anomaly as a trace of the upwelling lower mantle. *Nature* 336, 667–670. doi: 10.1038/336667a0
- Castillo, P. R. (2008). The origin of the adakite - high-Nb basalt association and its implications for post-subduction magmatism in Baja California, Mexico. *Geol. Soc. Am. Bull.* 120, 451–462. doi: 10.1130/B26166.1
- Castillo, P. R. (2013). A new hypothesis for the origin of HIMU and FOZO mantle end-members. *Min. Mag.* 77:838. doi: 10.1180/minmag.2013.077.5.3
- Castillo, P. R., Hilton, D. R., Halldórsson, S. A., and Wang, R. M. (2012). “T43C-2687: the geochemical and Sr-Nd-Pb-He isotopic characterization of the mantle source of Rungwe Volcanic Province: comparison with the Afar mantle domain,” in *Fall 2012 AGU Meeting* (San Francisco, CA).
- Chakrabarti, R., Basu, A. R., Santo, A. P., Tedesco, D., and Vaselli, O. (2009). Isotopic and geochemical evidence for a heterogeneous mantle plume origin of the Virunga volcanics, Western rift, East African Rift system. *Chem. Geol.* 259, 273–289. doi: 10.1016/j.chemgeo.2008.11.010
- Chazot, G., and Bertrand, H. (1993). Mantle sources and magma-continental crust interactions during early Red Sea-Gulf of Aden rifting in southern Yemen: elemental and Sr, Nd, Pb isotope evidence. *J. Geophys. Res.* 98, 1819–1835. doi: 10.1029/92JB02314
- Chernet, T., and Hart, W. K. (1999). Petrology and geochemistry of volcanism in the northern Main Ethiopian Rift – southern Afar transition region. *Acta Vulcanol.* 11, 21–41.
- Class, C., Goldstein, S. L., Stute, M., Kurz, M. D., and Schlosse, P. (2005). Grand Comore Island: a well-constrained “low $^3\text{He}/^4\text{He}$ ” mantle plume. *Earth Planet. Sci. Lett.* 233, 391–409. doi: 10.1016/j.epsl.2005.02.029
- Courtillot, V., Davaille, A., Besse, J., and Stock, J. (2003). Three distinct types of hotspots in the Earth's mantle. *Earth Planet. Sci. Lett.* 205, 295–308. doi: 10.1016/S0012-821X(02)01048-8
- Craig, H., Lupton, J. E., and Horowitz, R. (1977). Isotopic geochemistry and hydrology of geothermal waters in the Ethiopian Rift Valley. *Scripps Inst. Oceanogr. Tech. Rep.* 140, 77–14.
- Davies, G. R., and Lloyd, F. E. (1989). “Pb–Sr–Nd isotope and trace element data bearing on the origin of the potassic subcontinental lithosphere beneath southwest Uganda, Kimberlites and related rocks,” *Geol. Soc. Australia Sp. Pub.* 14 (Perth: Blackwell), 784–794.
- De Mulder, M., Hertogen, J., Deutsch, S., and Andre, L. (1986). The role of crustal contamination in the potassic suite of the Karisimbi Volcano (Virunga, African Rift Valley). *Chem. Geol.* 57, 117–136. doi: 10.1016/0009-2541(86)90097-5
- Dupuy, C., Liotard, J. M., and Dostal, J. (1992). Zr/Hf fractionation in intraplate basaltic rocks: carbonate metasomatism in the mantle source. *Geochim. Cosmochim. Acta* 56, 2417–2424. doi: 10.1016/0016-7037(92)90198-R
- Ebinger, C. J., Deino, A. L., Drake, R. A., and Tesha, A. L. (1989). Chronology of volcanism and rift basin propagation: Rungwe volcanic province, East Africa. *J. Geophys. Res.* 94, 15785–15803. doi: 10.1029/JB094iB11p15785

- Ebinger, C. J., and Sleep, N. H. (1998). Cenozoic magmatism throughout east Africa resulting from impact of a single plume. *Nature* 395, 788–791. doi: 10.1038/27417
- Fischer, T. P., Burnard, P., Marty, B., Hilton, D. R., Füre, E., Palhof, F., et al. (2009). Upper–mantle volatile chemistry at Oldoinyo Lengai volcano and the origin of carbonatites. *Nature* 459, 77–80. doi: 10.1038/nature07977
- Foley, S. F., Link, K., Tiberindw, J. B., and Barifajio, E. (2012). Patterns and origin of igneous activity around the Tanzanian craton. *J. Afr. Earth Sci.* 62, 1–18. doi: 10.1016/j.jafrearsci.2011.10.001
- Furman, T. (1995). Melting of metasomatized subcontinental lithosphere: undersaturated mafic lavas from Rungwe, Tanzania. *Contrib. Mineral. Petrol.* 122, 97–115. doi: 10.1007/s004100050115
- Furman, T. (2007). Geochemistry of East African Rift basalts: an overview. *J. Afr. Earth Sci.* 48, 147–160. doi: 10.1016/j.jafrearsci.2006.06.009
- Furman, T., and Graham, D. (1999). Erosion of lithospheric mantle beneath the East African Rift system: geochemical evidence from the Kivu volcanic province. *Lithos* 48, 237–262. doi: 10.1016/S0024-4937(99)00031-6
- Furman, T., Kaleta, K. M., Bryce, J., and Hanan, B. B. (2006). Tertiary mafic lavas of Turkana, Kenya: constraints on East African plume structure and the occurrence of high-m volcanism in Africa. *J. Petrol.* 47, 1221–1244. doi: 10.1093/petrology/eg009
- Gautheron, C., and Moreira, M. (2002). Helium signature of the subcontinental lithospheric mantle. *Earth Planet. Sci. Lett.* 199, 39–47. doi: 10.1016/S0012-821X(02)00563-0
- George, R., and Rogers, N. (2002). Plume dynamics beneath the African plate inferred from the geochemistry of the Tertiary basalts of southern Ethiopia. *Cont. Min. Petrol.* 144, 286–304. doi: 10.1007/s00410-002-0396-z
- George, R., Rogers, N., and Kelley, S. (1998). Earliest magmatism in Ethiopia: evidence for two mantle plumes in one flood basalt province. *Geology* 26, 923–926.
- Gill, J. B. (1981). *Orogenic Andesites and Plate Tectonics*. Berlin: Springer Verlag.
- Graham, D. W., Reid, M. R., Jordan, B. T., Grunder, A. L., Leeman, W. P., and Lupton, J. E. (2009). Mantle source provinces beneath the northwestern USA delimited by helium isotopes in young basalts. *J. Volcanol. Geotherm. Res.* 188, 128–140. doi: 10.1016/j.jvolgeores.2008.12.004
- Halldórsson, S. A., Hilton, D. R., Scarsi, P., Abebe, T., and Hopp, J. (2014). A common mantle plume source beneath the entire East African Rift System revealed by coupled helium–neon systematics. *Geophys. Res. Lett.* 41, 2304–2311. doi: 10.1002/2014GL059424
- Hanan, B. B., and Graham, D. W. (1996). Lead and helium isotope evidence from oceanic basalts for a common deep source of mantle plumes. *Science* 272, 991–995. doi: 10.1126/science.272.5264.991
- Hansen, S., Nyblade, A., and Benoit, M. (2012). Mantle structure beneath Africa and Arabia from adaptively parameterized P-wave tomography: implications for the origin of Cenozoic Afro–Arabian tectonism. *Earth Planet. Sci. Lett.* 319–320, 23–34. doi: 10.1016/j.epsl.2011.12.023
- Harkin, D. A. (1960). *The Rungwe Volcanics at the Northern End of Lake Nyasa*. Dar Es Salam: Geol. Surv. Tanganyika Mem. II.
- Hart, S. R. (1988). Heterogeneous mantle domains—Signatures, genesis and mixing chronologies. *Earth Planet. Sci. Lett.* 90, 273–296. doi: 10.1016/0012-821X(88)90131-8
- Hart, S. R., Hauri, E. H., Oschmann, L. A., and Whitehead, J. A. (1992). Mantle plumes and entrainment: isotopic evidence. *Science* 256, 517–520. doi: 10.1126/science.256.5056.517
- Hart, W. K., Woldegabriel, G., Walter, R. C., and Mertzman, S. A. (1989). Basaltic volcanism in Ethiopia: constraints on continental rifting and mantle interactions. *J. Geophys. Res.* 94, 7731–7748. doi: 10.1029/JB094iB06p07731
- Hilton, D. R., Grönvold, K., Macpherson, C. G., and Castillo, P. R. (1999). Extreme $^3\text{He}/^4\text{He}$ ratios in northwest Iceland: constraining the common component in mantle plumes. *Earth Planet. Sci. Lett.* 173, 53–60. doi: 10.1016/S0012-821X(99)00215-0
- Hilton, D. R., Halldórsson, S. A., Barry, P. H., T., Fischer, T. P., de Moor, J. M., Ramirez, C. J., et al. (2011). Helium isotopes at Rungwe Volcanic Province, Tanzania, and the origin of East African Plateaux. *Geophys. Res. Lett.* 38, L21304. doi: 10.1029/2011GL049589
- Hilton, D. R., Thirlwall, M. F., Taylor, R. N., Murton, B. J., and Nichols, A. (2000). Controls on magmatic degassing along the Reykjanes Ridge with implications for the helium paradox. *Earth Planet. Sci. Lett.* 183, 43–50. doi: 10.1016/S0012-821X(00)00253-3
- Hofmann, A., Farnetani, C. G., Spiegelman, M., and Class, C. (2011). Displaced helium and carbon in the Hawaiian plume. *Earth Planet. Sci. Lett.* 312, 226–236. doi: 10.1016/j.epsl.2011.09.041
- Hofmann, A. W. (1997). Mantle geochemistry: the message from oceanic volcanism. *Nature* 385, 219–229. doi: 10.1038/385219a0
- Hofmann, C., Courtillot, V., Feraud, G., Rouchett, P., Yirgu, G., Ketefo, E., et al. (1997). Timing of the Ethiopian flood basalt event and implications for plume birth and global change. *Nature* 389, 838–841. doi: 10.1038/39853
- Jackson, M. G., Hart, S. R., Koppers, A. A. P., Staudigel, H., Konter, J., Blusztajn, J., et al. (2007). The return of subducted continental crust in Samoan lavas. *Nature* 448, 684–687. doi: 10.1038/nature06048
- Janney, P. E., and Castillo, P. R. (1997). Geochemistry of Mesozoic Pacific MORB: constraints on melt generation and the evolution of the Pacific upper mantle. *J. Geophys. Res.* 102, 5207–5229. doi: 10.1029/96JB03810
- Lloyd, F. E., Huntingdon, A. T., Davies, G. R., and Nixon, P. H. (1991). “Phanerozoic volcanism of southwest Uganda: a case for regional K and LILE enrichment of the lithosphere beneath a domed and rifted continental plate,” in *Magmatism in Extensional Structural Settings: the Phanerozoic African Plate*, eds A. B. Kampunzu and R. T. Lubala (Berlin: Springer-Verlag), 23–72. doi: 10.1007/978-3-642-73966-8_3
- Lucassen, F., Franz, G., Romer, R. L., Pudlo, D., and Dulski, P. (2008). Nd, Pb, and Sr isotope composition of Late Mesozoic to Quaternary intra-plate magmatism in NE-Africa (Sudan, Egypt): high- μ signatures from the mantle lithosphere. *Contrib. Mineral. Petrol.* 156, 765–784. doi: 10.1007/s00410-008-0314-0
- Marty, B., Pik, R., and Yirgu, G. (1996). Helium isotopic variations in Ethiopian plume lavas: nature of magmatic sources and limit on lower mantle contribution. *Earth Planet. Sci. Lett.* 144, 223–237. doi: 10.1016/0012-821X(96)00158-6
- Montelli, R., Nolet, G., Dahlen, F., and Masters, G. (2006). A catalogue of deep mantle plumes: new results from finite–frequency tomography. *Geochim. Geophys. Geosyst.* 7:Q11007. doi: 10.1029/2006GC001248
- Nyblade, A. A. (2011). The upper-mantle low-velocity anomaly beneath Ethiopia, Kenya, and Tanzania: Constraints on the origin of the African superswell in eastern Africa and plate versus plume models of mantle dynamics. *Geol. Soc. Am.* 478, 37–50. doi: 10.1130/2011.2478(03)
- Nyblade, A. A., Owens, T. J., Gurrrola, H., Ritsema, J., and Langston, C. A. (2000). Seismic evidence for a deep upper mantle thermal anomaly beneath east Africa. *Geology* 28, 599–602. doi: 10.1130/0091-7613(2000)28<599:SEFADU>2.0.CO;2
- Pearce, J. A., Bender, J. F., De Long, S. E., Kidd, W. S. F., Low, P. J., Guñer, Y. et al., (1990). Genesis of collision volcanism in eastern Anatolia Turkey. *J. Volcanol. Geotherm. Res.* 44, 189–229. doi: 10.1016/0377-0273(90)90018-B
- Pik, R., Deniel, C., Coulon, C., Yirgu, G., and Marty, B. (1999). Isotopic and trace element signatures of Ethiopian flood basalts; evidence for plume–lithosphere interactions. *Geochim. Cosmochim. Acta* 63, 2263–2279. doi: 10.1016/S0016-7037(99)00141-6
- Pik, R., Marty, B., and Hilton, D. R. (2006). How many mantle plumes in Africa? The geochemical point of view. *Chem. Geol.* 226, 100–114. doi: 10.1016/j.chemgeo.2005.09.016
- Rogers, N., Macdonald, R., Fitton, J. G., George, R., Smith, M., and Barreiro, B. (2000). Two mantle plumes beneath the East African rift system: Sr, Nd and Pb isotope evidence from Kenya Rift basalts. *Earth Planet. Sci. Lett.* 176, 387–400. doi: 10.1016/S0012-821X(00)00012-1
- Rogers, N. W. (2006). Basaltic magmatism and the geodynamics of the East African Rift. *Geol. Soc. Spec. Publ.* 259, 77–93. doi: 10.1144/GSL.SP.2006.259.01.08
- Rogers, N. W., De Mulder, M., and Hawkesworth, C. J. (1992). An enriched mantle source for potassic basanites: evidence from Karisimbi volcano, Virunga volcanic province, Rwanda. *Cont. Mineral. Petrol.* 111, 543–556. doi: 10.1007/BF00320908
- Rogers, N. W., James, D., Kelley, S. P., and De Mulder, M. (1998). The generation of potassic lavas from the eastern Virunga province, Rwanda. *J. Petrol.* 39, 1223–1247. doi: 10.1093/petroj/39.6.1223
- Rooney, T. O., Hanan, B. B., Graham, D. W., Furman, T., Blichert-Toft, J., and Schilling, J.-G. (2012). Upper mantle pollution during Afar Plume – continental Rift Interaction. *J. Petrol.* 53, 365–389. doi: 10.1093/petrology/egr065
- Rooney, T. O., Hanan, B. B., Graham, D. W., Furman, T., Blichert-Toft, J., and Schilling, J.-G. (2014). The role of continental lithosphere metasomes in the production of HIMU-like magmatism on the northeast African and Arabian plates. *Geology* 42, 419–422. doi: 10.1130/G35216.1

- Rooney, T. O., Herzberg, C., and Bastow, I. D. (2011). Elevated mantle temperature beneath East Africa. *Geology* 40, 27–30. doi: 10.1130/G32382.1
- Rosenthal, A., Foley, S. F., Pearson, D. G., Nowell, G. M., and Tappe, S. (2009). Petrogenesis of strongly alkaline primitive volcanic rocks at the propagating tip of the western branch of the East African Rift. *Earth Planet. Sci. Lett.* 284, 236–248. doi: 10.1016/j.epsl.2009.04.036
- Rudnick, R. L., McDonough, W. F., and Chappell, B. W. (1993). Carbonatite metasomatism in the northern Tanzanian mantle: petrographic and geochemical characteristics. *Earth Planet. Sci. Lett.* 114, 463–475. doi: 10.1016/0012-821X(93)90076-L
- Scarsi, P., and Craig, H. (1996). Helium isotope ratios in Ethiopian Rift basalts. *Earth Planet. Sci. Lett.* 144, 505–516. doi: 10.1016/S0012-821X(96)00185-9
- Shinjo, R., Chekol, T., Meshesha, D., Itaya, T., and Tatsumi, Y. (2011). Geochemistry and geochronology of the mafic lavas from the southeastern Ethiopian rift (the East African Rift System): assessment of models on magma sources, plume–lithosphere interaction and plume evolution. *Contrib. Mineral. Petrol.* 162, 209–230. doi: 10.1007/s00410-010-0591-2
- Stewart, K., and Rogers, N. (1996). Mantle plume and lithosphere contributions to basalts from southern Ethiopia. *Earth Planet. Sci. Lett.* 139, 195–211. doi: 10.1016/0012-821X(96)00015-5
- Stracke, A., Hofmann, A. W., and Hart, S. R. (2005). FOZO, HIMU, and the rest of the mantle zoo. *Geochem. Geophys. Geosys.* 6, Q05007. doi: 10.1029/2004GC000824
- Sun, S.-S., and McDonough, W. F. (1989). “Chemical and isotopic systematics of oceanic basalts: implications for mantle composition and processes,” in *Magmatism in the Ocean Basins*, Vol.42, eds A. D. Saunders and M. J. Norry (London: Sp. Pub), 313–345. doi: 10.1144/GSL.SP.1989.042.01.19
- Thirlwall, M. F. (1997). Pb isotopic and elemental evidence for OIB derivation from young HIMU mantle. *Chem. Geol.* 139, 51–74. doi: 10.1016/S0009-2541(97)00033-8
- Thirlwall, M. F. (2000). Inter-laboratory and other errors in Pb isotope analyses investigated using a ^{207}Pb – ^{204}Pb double-spike. *Chem. Geol.* 163, 299–322. doi: 10.1016/S0009-2541(99)00135-7
- Tian, L., Castillo, P. R., Hawkins, J. W., Hilton, D. R., Hanan, B. B., and Pietruszka, A. A. (2008). Major and trace element and Sr–Nd isotope signatures of the mantle beneath the Central Lau Basin: implications for the nature and influence of subduction components. *J. Volcanol. Geotherm. Res.* 178, 657–670. doi: 10.1016/j.jvolgeores.2008.06.039
- Trua, T., Deniel, C., and Mazzuoli, R. (1999). Crustal control in the genesis of Plio-Quaternary bimodal magmatism of the Main Ethiopian Rift (MER): geochemical and isotopic (Sr, Nd, Pb) evidence. *Chem. Geol.* 155, 201–231. doi: 10.1016/S0009-2541(98)00174-0
- Vollmer, R., and Norry, M. J. (1983a). Unusual isotopic variations in Nyiragongo nephelinites. *Nature* 301, 141–143. doi: 10.1038/301141a0
- Vollmer, R., and Norry, M. J. (1983b). Possible origin of K-rich volcanic rocks from Virunga, East Africa, by metasomatism of continental crust material: Pb, Nd and Sr isotopic evidence. *Earth Planet. Sci. Lett.* 64, 374–386. doi: 10.1016/0012-821X(83)90097-3
- White, W. M. (2010). Oceanic island basalts and mantle plumes: the geochemical perspective. *Ann. Rev. Earth Planet. Sci.* 38, 133–160. doi: 10.1146/annurev-earth-040809-152450
- WoldeGabriel, G., Aronson, J. L., and Walter, R. C. (1990). Geology, geochronology, and rift basin development in the central sector of the Main Ethiopia Rift. *Geol. Soc. Am. Bull.* 102, 439–458.
- Wolfenden, E., Ebinger, C., Yirgu, G., Deino, A., and Ayalew, D. (2004). Evolution of the northern Main Ethiopian rift: birth of a triple junction. *Earth Planet. Sci. Lett.* 224, 213–228. doi: 10.1016/j.epsl.2004.04.022

Conflict of Interest Statement: The authors declare that the research was conducted in the absence of any commercial or financial relationships that could be construed as a potential conflict of interest.

Received: 03 June 2014; paper pending published: 20 July 2014; accepted: 20 August 2014; published online: 08 September 2014.

Citation: Castillo PR, Hilton DR and Halldórsson SA (2014) Trace element and Sr–Nd–Pb isotope geochemistry of Rungwe Volcanic Province, Tanzania: implications for a Superplume source for East Africa Rift magmatism. *Front. Earth Sci.* 2:21. doi: 10.3389/feart.2014.00021

This article was submitted to Petrology, a section of the journal *Frontiers in Earth Science*.

Copyright © 2014 Castillo, Hilton and Halldórsson. This is an open-access article distributed under the terms of the Creative Commons Attribution License (CC BY). The use, distribution or reproduction in other forums is permitted, provided the original author(s) or licensor are credited and that the original publication in this journal is cited, in accordance with accepted academic practice. No use, distribution or reproduction is permitted which does not comply with these terms.